REVIEW

Electrospun Metal–Organic Framework Nanofiber Membranes for Energy Storage and Environmental Protection

Xiaoge Liu[1] · Yi Zhang[1] · Xiaotian Guo[1] · Huan Pang[1]

Abstract

Metal–organic frameworks (MOFs) are attractive in many fields due to their unique advantages. However, the practical applications of single MOF materials are limited. In recent years, a large number of MOF-based composites have been investigated to overcome the defects of single MOF materials to broaden the avenues for the practical applications of MOFs. Among them, MOF-based hybrid nanofiber membranes fabricated by electrospinning combine the advantages of polymer nanofibers and inorganic porous materials, receiving extensive attention and development in energy storage and environmental protection. This review systematically summarizes the recent progress of MOF-based hybrid nanofiber membranes prepared by electrospinning from the perspectives of preparation and application. Firstly, two main methods for preparing MOF/polymer nanofibrous membranes are discussed. Next, the applications of MOF/polymer nanofibrous membranes in energy storage and environmental protection are summarized at length. Finally, to fully tap the potential of MOF-based nanofiber membranes in more fields, the current challenges are proposed, and future research directions are discussed.

Keywords Metal–organic framework · Electrospun · Energy storage · Environmental protection

Introduction

Global population, economic growth, and energy consumption have led to a marked increase in carbon dioxide and other gas emissions [1–6]. Additionally, the problem of water pollution cannot be ignored. Pollutants from wastewater, such as heavy metals, dyes, etc., can bring out severe damage to humans and even endanger lives [7–10]. Based on the above problems, it is particularly imperative to develop materials with excellent performance for energy storage and environmental protection [11–13]. In this connection, various technologies have been developed to realize the devices with high performance for energy storage and environmental protection [14–17]. Common functional materials with porosity, such as zeolites, porous polymers, active carbon and MOFs, have made significant contributions to energy storage and environmental protection [18–23].

Among the above-mentioned functional materials, MOFs are considered to possess great potential for energy and environmental applications owing to their large specific surface area, flexible skeleton and tunable pore sizes [24–31]. MOFs are a new type of porous crystalline materials composed of organic ligands and inorganic metal ions [32–36]. Compared with conventional porous materials, MOFs have a remarkable feature of controlling their structure and composition by employing appropriate metal ions and organic ligands [37–40]. Hence, MOFs possess the characteristics of various designs, controllable structures, simple fabrication, adjustable functions, flexible frameworks, and so on, all of which are attributed to the promising precursors for the preparation of advanced materials with outstanding properties [41–50]. Due to the merits above, MOFs have become candidates for applications in many fields, including supercapacitors, batteries, wastewater treatment, sensors, air pollution filtration, and so forth [51–61]. However, due to the inherent defects of MOFs (such as traditional morphologies and processing difficulties), single MOF materials can hardly satisfy the requirements of practical applications [62–64]. To solve these problems, researchers have done many studies on MOF composites. MOF composites formed by combining MOFs with other functional materials (such as polymers,

✉ Huan Pang
panghuan@yzu.edu.cn; huanpangchem@hotmail.com

1 School of Chemistry and Chemical Engineering, Yangzhou University, Yangzhou 225002, Jiangsu, People's Republic of China

nanoparticles, carbon substrates, conductive substrates) possess physico-chemical properties that the pristine MOFs cannot provide, such as excellent electrical conductivity, mechanical stability, and catalytic performance. In recent years, a large number of MOF composites have exhibited outstanding stability and excellent physico-chemical properties under harsh environment (highly acid/highly alkali). By introducing suitable polymers and necessary molding techniques, MOF composites are expected to play an important role in energy storage and environmental protection [65]. MOFs are usually synthesized by traditional solvothermal or hydrothermal methods. At the same time, polymers as adhesives can not only enhance the mechanical flexibility of composites, but also ensure the chemical stability of materials. The membrane materials formed by combining MOFs with polymer-carriers have the characteristics of integrity, porosity and flexibility, which can effectively expand the practical applications of MOFs thanks to the combination of the advantages of porous nanoparticles and polymers [66–68].

Electrospinning is a proven and effective method for the direct and continuous preparation of polymer nanofibers [69–75]. Due to the advantages of stable performance, excellent quality, comprehensive spinnable materials and controllable process, it has an extensive application prospect in energy storage and environmental protection [76–90].

In recent years, MOF-based electrospun polymer nanofiber membranes have been widely used in gas sensing, gas separation, air pollution filtration, energy storage, and wastewater treatment [13, 91–101]. MOF/polymer electrospun nanofiber membranes exhibit the following advantages: (I) owing to the outstanding permeability and excellent mechanical strength of polymer electrospun nanofibers, they are considered the ideal frame structure to support MOF particles. These features facilitate the transformation of MOF nanoparticles into self-supporting MOF-based nanofibrous membranes; (II) MOF/polymer composite fibers combine the merits of MOF nanoparticles with various crystal structures as well as synthetic physicochemical properties and electrospun nanofibers, e.g., outstanding flexibility, controllable morphology and lightweight, which are beneficial to commendably realize the synergistic effect and thoroughly expand the applications of the two materials [102–107]; (III) the combination of MOF and electrospinning nanofibers can mitigate the misgivings that particles are easy to agglomerate and difficult to recycle [56, 65, 108, 109]. Consequently, MOF/polymer nanofiber membranes are considered as available functional materials to expand the applications of MOFs, such as environmental protection and electrochemical energy storage [64, 110–116]. Hitherto, two main routes to fabricate MOF-loaded electrospun nanofiber membranes have been developed, namely "direct electrospinning" and "surface in situ growth." The direct electrospinning route requires only a simple three-step process: synthesis of MOF

powder nanoparticles, preparation of slurry by adding MOF nanoparticles into polymer solutions, and direct electrospun of the slurry. The prerequisite for the successful preparation of nanofiber membranes through this strategy is the chemical compatibility between MOF, polymer and solvent components. The preparation of MOF/polymer nanofiber membranes by surface in-situ growth strategy requires two steps: electrospun of a polymer nanofiber layer and evolution of MOF crystals in the open pores and on the surface of the nanofiber layer. This approach requires the use of relatively stable polymer nanofibers that can endure the preparation conditions of target MOF particles, which may need to consider the use of corrosive solvents or relatively high pressures and temperatures (solvothermal or hydrothermal conditions).

This review systematically summarizes the latest progress of MOF-based electrospun nanofiber membranes. Although there have been many reviews in this research field, the summary of the fabrication routes of MOF-based nanofiber membranes is still not very detailed. In this review, the preparation routes of MOF/polymer nanofiber membranes are illustrated, and the differences, advantages as well as disadvantages of direct electrospinning and surface in situ growth are introduced in detail, which is obviously different from other reviews. Next, the main applications of MOF/polymer nanofiber membranes in energy storage and environmental protection are discussed at length. Finally, the key challenges in the above fields are proposed, and some relevant ideas for future research are put forward. This review will provide essential insights into the rational design of electrospinning fibers for energy and environmental applications in the future and facilitate the development of more advanced functional materials in various industries.

Routes for the Fabrication of MOF/Polymer Nanofiber Membranes

MOF/polymer nanofiber membranes are generally acquired by electrospinning. Electrospinning is a unique nanofiber manufacturing process in which polymer solution systems are jet-spun under the action of high-voltage static electricity [117–120]. Numerous polymer solution systems have been widely used in electrospun, such as polyvinylpyrrolidone (PVP) in ethanol (EtOH), polyacrylonitrile (PAN) in N,N-dimethylformamide (DMF), polystyrene (PS) in tetrahydrofuran (THF). The nanofibers prepared by electrospinning possess the features of large specific surface area, high porosity, easy size control and surface functionalization (such as surface coating and surface modification). Thanks to these advantages, the prepared nanofibers exhibit excellent application value in many fields. Two main ways have been excavated for the fabrication of MOF/polymer fiber

membranes based on electrospun, which are direct electrospinning [121] and surface in situ growth [122]. Figure 1 displays the MOF/polymer nanofiber membranes prepared by these two routes. This section discusses the two routes for preparing MOF/polymer nanofiber membranes. The information on fabrication routes is summarized in Table 1.

Direct Electrospinning

MOF/polymer nanofiber membranes are generally prepared by direct electrospinning with a simple three-step preparation: synthesis of MOF powder nanoparticles, preparation of slurry by adding MOF nanoparticles into polymer solutions, and direct electrospun of the slurry [123]. The prerequisite for the successful preparation of nanofiber membranes is chemical compatibility between MOF, polymer and solvent components. Furthermore, the polymer/solvent system, the slurry performance and the electrospinning conditions are

optimized according to the specific application of the target MOF and polymer system [124, 125]. Therefore, MOF/polymer nanofiber membranes with different properties are fabricated.

MOF/polymer nanofibrous membranes can be successfully prepared by electrospinning of MOF/polymer slurries obtained by mixing MOF particles with different polymer/solvent systems. For instance, the supported microporous membranes prepared seminally by direct electrospinning were used for gas separation for the first time [123]. Well-grown and defect-free zeolitic imidazolate framework-8 (ZIF-8) membranes were successfully prepared using ZIF-8 nanoparticles to cover macroporous silica (SiO_2) support tubes with MOF/polymer fiber layers. The direct electrospun process of a mixed slurry of ZIF-8/PVP is shown schematically in Fig. 2a. Figure 2b displays the top-view of the ZIF-8/PVP nanofiber membranes. It shows that ZIF-8 crystals have a rhombic dodecahedron morphology, completely
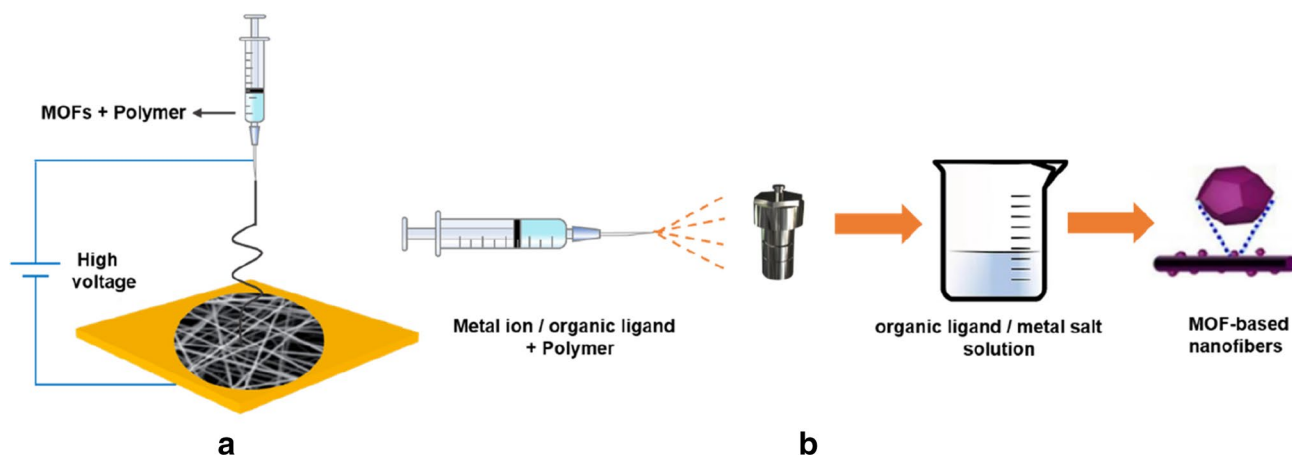

Fig. 1 **a** Direct electrospinning; **b** electrospun metal ion/polymer or ligand/polymer nanofibers followed by surface in situ growth of MOF particles

Table 1 Information about the fabrication routes of MOF/polymer electrospun fiber membranes

| MOF	Metal center	Ligand	Composite nanofibers	Route	References
ZIF-8	Zn	2-methylimidazole	ZIF-8/PVP	Direct electrospinning	[123]
ZIF-8	Zn	2-methylimidazole	ZIF-8/PI	Direct electrospinning	[126]
ZIF-8	Zn	2-methylimidazole	ZIF-8/PAN	Surface in situ growth (I)	[133]
ZIF-67	Co	2-methylimidazole	ZIF-67/PAN	Surface in situ growth (I)	[134]
ZIF-8	Zn	2-methylimidazole	ZIF-8/PAN	Surface in situ growth (II)	[105]
MIL-100	Fe	Trimesic acid	MIL-100/PAN	Surface in situ growth (II)	[135]
UiO-66-NH$_2$	Zr	Amino-terephthalic acid	UiO-66-NH$_2$/PAN	Surface in situ growth (II)	[136]
ZIF-8	Zn	2-methylimidazole	ZIF-8/PI	Surface in situ growth (III)	[137]
ZIF-8	Zn	2-methylimidazole	ZIF-8/PU	Surface in situ growth (III)	[138]
ZIF-8	Zn	2-methylimidazole	ZIF-8/ESF	Surface in situ growth (III)	[139]
ZIF-67	Co	2-methylimidazole	ZIF-67/ESF	Surface in situ growth (III)	[139]
UiO-66-NH$_2$	Zr	Amino-terephthalic acid	UiO-66-NH$_2$/ PAN	Surface in situ growth (III)	[140]
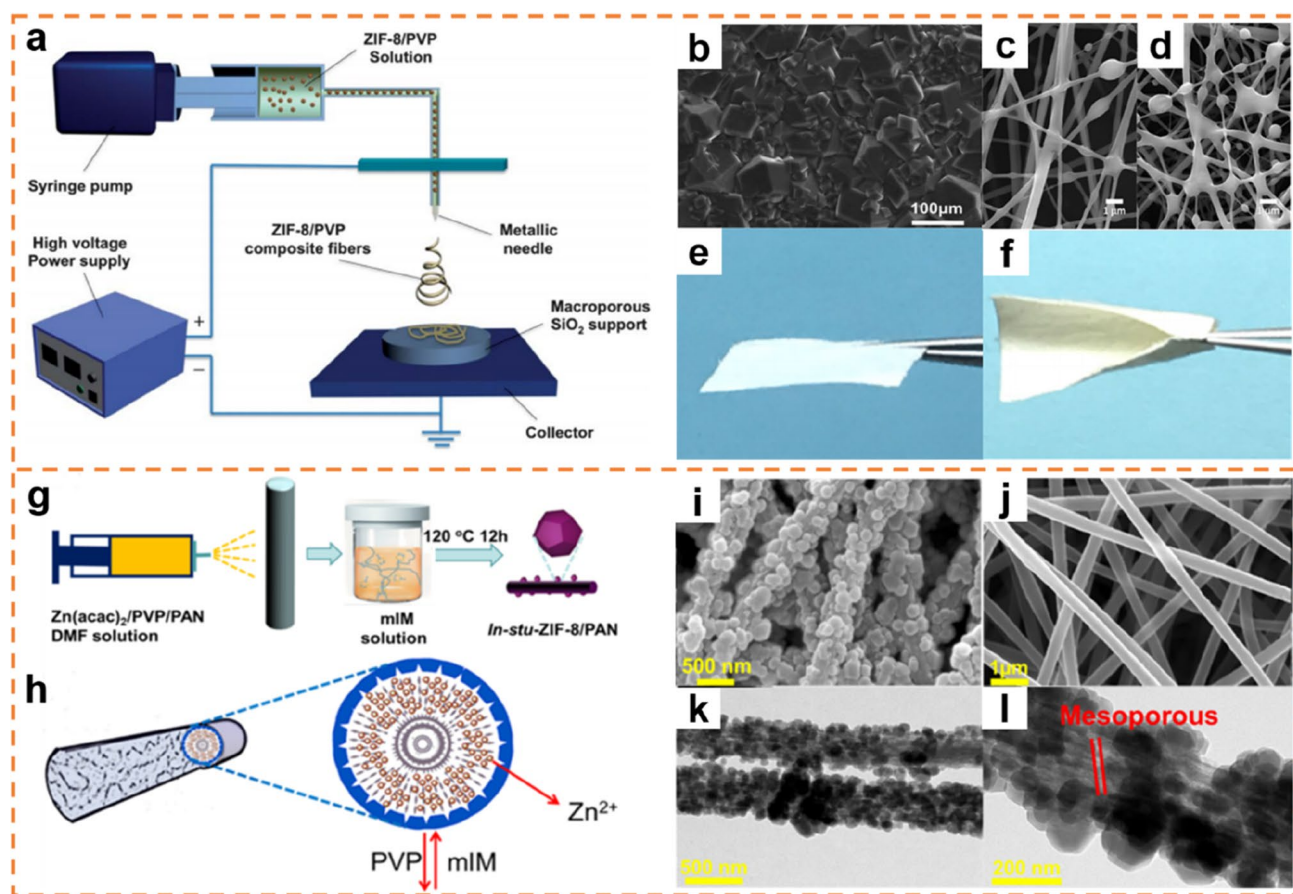
Fig. 2 a Schematic diagram of direct electrospinning process for ZIF-8/PVP fiber layers on macroporous SiO$_2$ support tubes; **b** top-view of the ZIF-8 membranes containing ZIF-8/PVP fibers. Reproduced with permission from Ref [123]. Copyright 2012, the Royal Society of Chemistry. SEM pictures of **c** PI and **d** ZIF-8/PI membranes after filtering PM$_{2.5}$ in the air; exhibition of ZIF-8/PI membrane **e** stiffness and **f** flexibility. Reproduced with permission from Ref [126]. Copyright 2019, American Chemical Society. **g** Schematic diagram of the in situ growth of ZIF-8 on electrospinning nanofibers; **h** formation mechanism of the in situ ZIF-8/PAN nanofibers; SEM images of **i** the in situ ZIF-8/PAN nanofibers and **j** PAN; **k**, **l** TEM images of the in situ ZIF-8/PAN nanofibers. Reproduced with permission from Ref [133]. Copyright 2018, American Chemical Society

coating the support surface and growing well, which proves that the composite membranes were defect-free. Similarly, the ZIF-8/polyimide (PI) nanofiber membranes were successfully prepared by direct electrospinning [126]. Figure 2 c and d reveal the microstructures of PI and ZIF-8/PI fiber membranes after filtering particulate matter with an aerodynamic diameter of less than 2.5 mm (PM$_{2.5}$), respectively. The ZIF-8/PI membranes exhibit excellent deformation resistance and independence owning to the high modulus in the initial stage of deformation (Fig. 2e). Simultaneously, the membranes with increased stiffness still maintain sufficient flexibility (Fig. 2f).

Surface In situ Growth

The activity and controllability of MOF-based nanofibrous membranes prepared by direct electrospinning are often limited in practical applications. Details are as follows. (I)

Because the MOF particles are embedded in the polymer nanofibrous membranes, the internal pores of the pristine MOF crystals tend to be coated by the polymer matrix, which greatly limits the activity of MOFs in most applications. (II) Excessive MOF crystals may affect the conductivity of the electrospinning solution, resulting in electrospinning failure. Therefore, the controllability of the amount of MOF nanoparticles introduced is very critical in practical applications.

The route of surface in situ growth can ideally overcome these drawbacks [127, 128]. The brilliance of this approach is that the internal and the surface pores of original MOF particles are not coated by polymer matrix and are commendably controllable. Moreover, the physicochemical properties of the MOF particles remain unchanged. MOF/polymer nanofiber membranes were fabricated initially by surface in situ growth with a simple two-step process: electrospun of a polymer nanofiber layer and evolution of

MOF crystals in the open pores and on the surfaces of the nanofiber layer [129, 130]. There are three main ways of surface in situ growth. They have similar growth paths and features, that is, polymer nanofiber membranes need to be immersed in the corresponding precursors. (I) Metal ions are brought into the polymer nanofibers by electrospun, and then the metal ions/polymer electrospinning nanofiber membranes are soaked in the organic ligand solution to load the target MOFs by surface in situ growth; (II) ligands are introduced in the polymer fibers by electrospun, and then the ligands/polymer electrospinning fiber membranes are soaked in the metal salt solution to load MOF nanocrystals, and (III) MOF crystals are grown directly on the surface of polymer electrospun nanofiber membranes containing some nucleation sites [131, 132]. These three in situ growth routes are not only feasible and simple, but also effectively avoid the problem of poor compatibility between MOFs and polymers. However, these three paths also have limitations. For example, (I) the relatively stable polymer nanofibers are supposed to be used to ensure that they can withstand the preparation conditions of the target MOF particles, which may require consideration of the employment of aggressive solvents or relatively high pressures and temperatures (solvothermal or hydrothermal conditions); (II) the nucleation of MOF crystals is difficult to control, resulting in the shedding of the grown MOFs and the difficulty in controlling the crystal thickness; (III) the reaction temperature, reaction time and concentration of the precursor solution are supposed to be appropriate for MOF nanoparticles growth. These three growth paths are discussed in detail below.

Metal Ion/Polymer Electrospun

The metal ion is brought into polymer nanofibers by electrospun, and then MOF nanocrystals load on fibers by immersing metal ion/polymer into ligand solution. There are many works to fabricate nanofibers based on this approach, which pave the way for the great development of MOF-based fiber membranes. For example, the ZIF-8-based polymer nanofiber (ZIF-8/PAN) membranes fabricated seminally by surface in situ growth have been reported, and the preparation process is illustrated in Fig. 2g [133]. Firstly, the mixture of PVP and PAN was added into the $Zn(acac)_2$ solution to obtain the spinning precursor. Then, the $Zn(acac)_2$/PVP/PAN nanofibers fabricated by electrospinning were soaked into a 2-methylimidazole (mIM) solution to obtain ZIF-8/PAN nanofiber membranes. PVP is easier to dissociate from composite nanofibers under hydrothermal conditions because PVP is more hydrophilic than PAN (Fig. 2h). In situ growth of a homogeneous ZIF-8 crystal layer on the nanofibers' surface was confirmed by scanning electron microscopy (SEM) characterization, and the surface of the fibers with ZIF-8 crystals (Fig. 2i) was rougher than that

of the fibers without ZIF-8 crystals (Fig. 2j). Furthermore, transmission electron microscopy (TEM) characterization demonstrated that ZIF-8 crystals grew not only on the surface of the nanofibers, but also inside the PAN fibers by in situ growth (Fig. 2 k and l). And the high magnification TEM picture brought the mesoporous structure of ZIF-8/PAN fibers into sight (Fig. 2l). Similar research was pointed out by Bian et al. [134] They prepared $Co(AC)_2$/PAN fiber membranes by electrospun and then immersed the composite fiber membranes into mIM solution dissolved in ethanol at room temperature to incorporate ZIF-67 crystals into the $Co(AC)_2$/PAN electrospun membranes by surface in situ growth. As depicted in Fig. 3a, ZIF-67/PAN electrospun fiber membranes were finally obtained. Interestingly, a layer of evenly distributed ZIF-67 crystals was observed on the surface of the nanofiber membranes by SEM (Fig. 3b–g) and TEM (Fig. 3h–j), which made the surface of the fiber rougher. Introducing metal ions into nanofibers by electrospinning and then obtaining uniformly dispersed MOF particles by in situ growth is simple and easy to operate. It plays an important role in the preparation of polymer nanofibers.

Ligand/Polymer Electrospun

Immersing ligand/polymer substrates prepared by electrospinning into a metal salt solution to grow MOF particles by in situ generation has been widely used to fabricate electrospun fiber membranes. Blending mIM solution in polymer nanofibers and then soaking the composite fibers into the solution of $Zn(OAc)_2$ $2H_2O$ dissolved in methanol to load MOF nanocrystals by in situ growth has been reported in detail by Ma et al. [105]. Figure 3k illustrates the synthesis procedures of ZIF-8/PAN fibers. From the microstructure of the composite (Fig. 3l), it can be concluded that ZIF-8 crystals grew along the nanofibers and adhered to the PAN substrate, which brought about stronger adhesion [123] and ideally overcame the difficulty of nanofiber surface pretreatment. Furthermore, the SEM images (Fig. 3m, n) intuitively demonstrated that the surface of the PAN substrate was coated with a layer of dense and homogenous ZIF-8 crystals [104], indicating that the ZIF-8/PAN electrospun fiber membranes were successfully prepared. Additionally, Zhao et al. immersed trimesic acid (H_3BTC)/PAN blend electrospun fiber membranes prepared by electrospinning into $FeCl_3$ solution dissolved in pure water [135]. They found that trimesic acids from H_3BTC/PAN fiber membranes acted as the nucleation sites for MIL-100(Fe) grown in situ on electrospun fibers during the hydrothermal reaction, and a compact and continuous layer of MIL-100 particles was grown in situ on the surface of the fiber membranes (Fig. 4a). As depicted in Fig. 4b, c, the PAN surface was coated entirely by the MIL-100 crystals, which grew along the nanofibers and were well-aligned after a two-step process. According
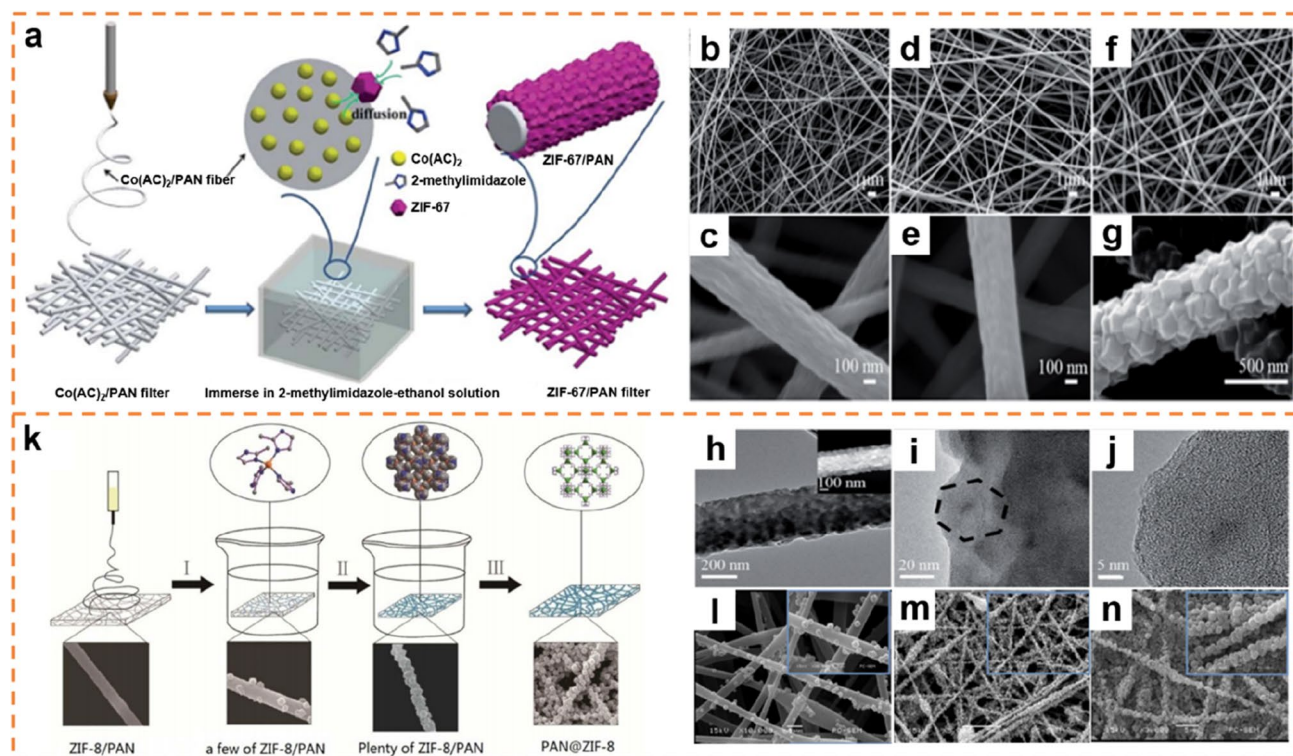
Fig. 3 a Schematic diagram of the in situ growth of ZIF-67 on electrospinning fibers; SEM photographs of **b, c** the pure PAN fibers, **d, e** Co(AC)$_2$/PAN fibers, and **f, g** ZIF-67/PAN fibers; **h** dark-field and bright-field TEM photographs of the ZIF-67/PAN fibers; **i, j** high-resolution TEM photographs of the ZIF-67/PAN fibers. Reproduced with permission from Ref [134]. Copyright 2018, the Royal Society of Chemistry. **k** Schematic diagram of the fabrication procedures of PAN@ZIF-8 electrospinning fibers; SEM pictures of **l** ZIF-8 on the PAN and **m, n** the ZIF-8/PAN nanofibers. Reproduced with permission from Ref [105]. Copyright 2016, the Royal Society of Chemistry

to Liu et al., PAN electrospun fiber membranes blended with amino-terephthalic acid (ATA) ligands were soaked into a solution of ZrCl$_4$ dissolved in acetone, and a uniform layer of UiO-66-NH$_2$ particles was evenly grown in situ on the surface of fiber membranes with ATA ligands acted as the nucleation sites under solvothermal conditions, as shown in Fig. 4d–g [136].

MOF/Polymer Electrospun

Due to the distinct chemical properties of MOF and polymers, it is difficult to achieve direct bonding between MOF and polymer surfaces. To solve this problem, serving polymer nanofiber membranes containing nucleation sites (such as carboxyl) as the substrate, MOF crystals are grown in situ on the surface of nanofiber membranes through the interaction between nucleation sites from electrospinning nanofiber membranes and metal ions from MOFs, which can provide outstanding load efficiency for MOFs. The driving forces for the growth of MOF crystals mainly come from the interaction between specific functional groups. The ideal in situ growth of ZIF-8 crystals can be achieved on the surface of PI electrospun fiber membranes [137]. The surface of PI fiber

membranes contains a large number of carboxyl groups, which can form a hydrogen bonding interaction with the imino groups from the ligand (mIM) of ZIF-8. It can be seen from SEM that ZIF-8 crystals were uniformly loaded on PI electrospun membranes. Zhou et al. took polyurethane (PU) electrospun fiber membranes with concentrated chromic anhydride and sulfuric acid-functionalized surface as the growth substrate of ZIF-8 (Fig. 5a) [138]. The functionalized fiber surface increased the binding sites, which was favorable for the fibers to capture Zn^{2+}. Figure 5b–e reveals the SEM images for in situ growth of ZIF-8 on PU. A strategy to fabricate electrospun-silk-nanofiber (ESF) membranes containing a layer of dense and uniform ZIF-8 or ZIF-67 crystals was proposed by Li et al. [139] Compared with the conventional polymer fiber membranes, the density and amount of MOF crystals loaded on the surface of fibers were obviously improved owing to the arrangement of binding and nucleation sites on the ESF membranes. In other findings, the electrospinning PAN fiber membranes soaked into NaOH and HCl solutions sequentially were engaged in the solution of UiO-66-NH$_2$ for in situ generations [140]. The surface of PAN fiber membranes was covered with a layer of homogeneous UiO-66-NH$_2$ particles by the interaction
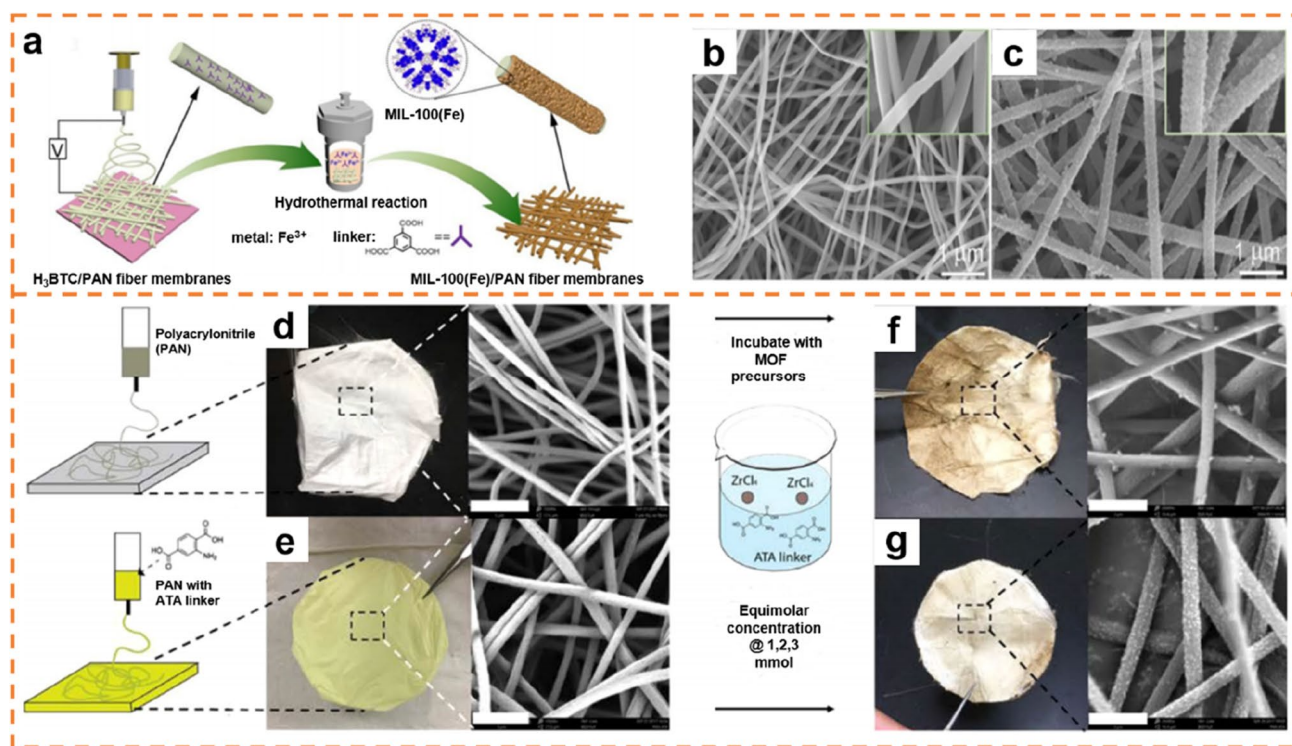
Fig. 4 a Schematic diagram of the fabrication of MIL-100/PAN fiber membranes. SEM pictures of b H$_3$BTC/PAN fiber membranes and c MIL-100/PAN fiber membranes. Reproduced with permission from Ref [135]. Copyright 2019, the Royal Society of Chemistry. Schematic diagram of the preparation of UiO-66-NH$_2$/PAN fiber membranes by in situ growth of UiO-66-NH$_2$ on electrospinning fibers: d control PAN sample; e PAN with ATA; f control PAN post-synthesis; g PAN with ATA post-synthesis. Reproduced with permission from Ref [136]. Copyright 2017, American Chemical Society

between the amino groups from the MOFs and the C=O bond from carboxyls on the surface of the fibers, as depicted in Fig. 5f.

Applications of MOF Nanofiber Membranes

MOF nanofibrous membranes play a significant role in energy [141–143] and environmental [144–148] applications. This section reviews the applications of MOF nanofiber membranes in energy storage and environmental protection, and summarizes such information in Table 2.

Batteries

Lithium-ion batteries (LIBs), lithium-sulfur batteries (LSBs) and sodium-ion batteries (SIBs) are the most widely used energy storage devices in our lives, which play an important role in mobile phones and computers [149]. Generally, the properties of the battery are determined by the electrode materials. Consequently, abundant researches have been conducted to explore excellent electrode materials with acceptable rate performance, high specific capacitance and outstanding cycle performance [150–154]. Thanks to the large specific surface area, hierarchical porous structure and exceptional conductivity of MOF derivatives (such as carbonized MOF nanofibers), they are considered as potential electrode material candidates.

Lithium-Ion Batteries

Carbonized MOF nanofibers are generally used as self-templates or precursors to develop porous metal oxides for electrode materials [155–159]. These materials can not only improve the pore size distribution and the specific surface area of the contact area between the electrolyte and the electrode, but also supply extra active centers to effectively reduce the diffusion path of lithium ions, bringing about the enhancement of the electrochemical properties [160–162].

Advanced anode materials for lithium storage have been intensively studied. For example, inspired by the high nitrogen (N) content and the porous structures of MOF derivatives, a strategy combining electrospinning and the subsequent hydrothermal reaction was designed to prepare Molybdenum disulfide (MoS$_2$) based nanofibers with a layered structure, in which thin MoS$_2$ nanosheets were vertically assembled on the N-doped porous carbon nanofibers (PCNFs) derived from PAN-MOF [115]. As visualized in
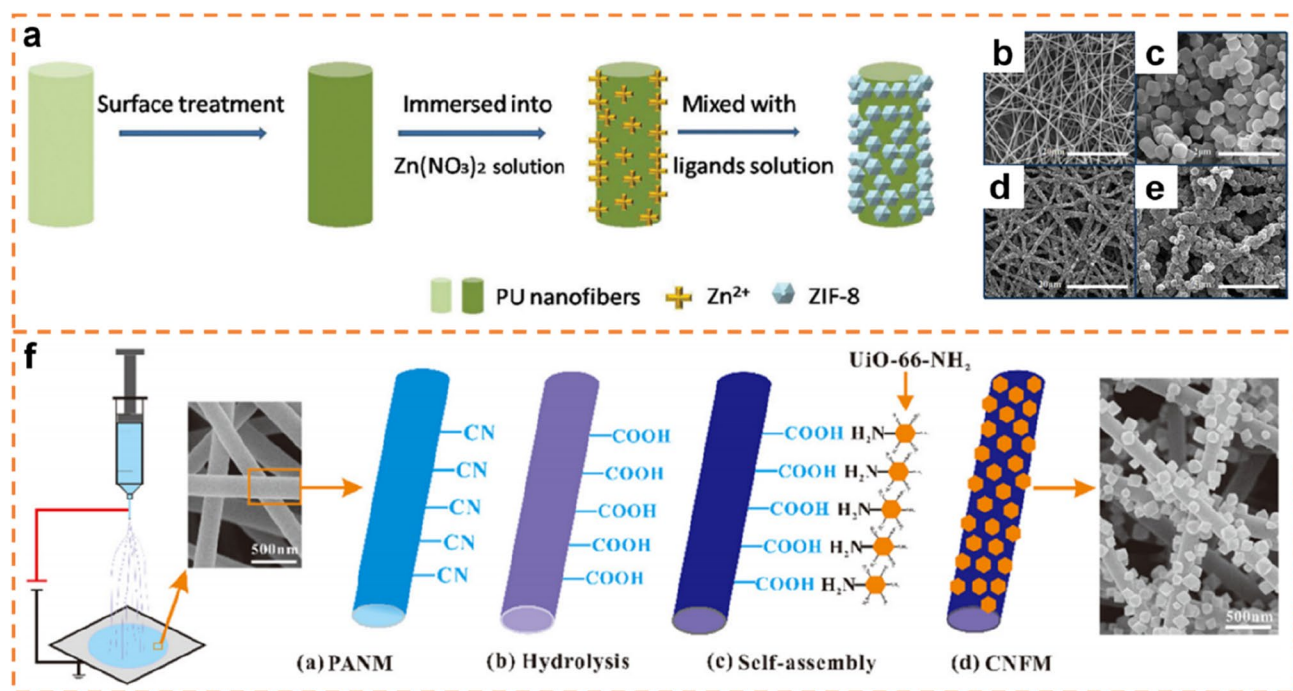
Fig. 5 **a** Schematic sketch for in situ growth of ZIF-8 crystals on PU fibers; SEM pictures for in situ growth of ZIF-8 on PU: **b** PU; **c** ZIF-8; **d**, **e** ZIF-8/PU. Reproduced with permission from Ref [138]. Copyright 2014, the Royal Society of Chemistry. **f** Schematic sketch of the fabrication of PAN fiber membrane covered with UiO-66-NH$_2$. Reproduced with permission from Ref [140]. Copyright 2019, Elsevier

Table 2 Information about the MOF/polymer electrospun fiber membranes for energy and environmental applications

MOF	Composite nanofibers	Route	Application	References
ZIF-8	ZIF-8/PAN	Direct electrospinning	Lithium-ion batteries	[115]
ZIF-67	ZIF-67/PAN	Surface in situ growth (I)	Lithium-ion batteries	[163]
ZIF-67	ZIF-67/PAN	Surface in situ growth (I)	Lithium-sulfur batteries	[175]
ZIF-67	ZIF-67/PAN	Direct electrospinning	Lithium-sulfur batteries	[176]
ZIF-8/ZIF-67	ZIF-8/ZIF-67/PAN	Surface in situ growth (II)	Sodium-ion batteries	[193]
MIL-88A(Fe)	MIL-88A/PAN	Surface in situ growth (III)	Sodium-ion batteries	[194]
MOF-808-EDTA	MOF-808-EDTA/PAN	Direct electrospinning	Heavy metal ions, oils	[205]
ZIF-67	ZIF-67/CA	Surface in situ growth (II)	Heavy metal ions	[206]
bio-MOF-1	bio-MOF/PAN	Direct electrospinning	Dyes	[212]
ZIF-8	ZIF-8@GO/PLA	Surface in situ growth (III)	Dyes	[213]
MIL-53(Al)–NH$_2$	MIL-53–NH$_2$/PAN	Surface in situ growth (III)	PM, SO$_2$, O$_3$	[220]
ZIF-8, UiO-66-NH$_2$, MOF-199, Mg-MOF-74	ZIF-8/PAN, UiO-66-NH$_2$, MOF-199/PAN, Mg-MOF-74/PAN	Direct electrospinning	PM$_{2.5}$, PM$_{10}$, SO$_2$	[221]
ZIF-8	ZIF-8/PI	Direct electrospinning	PM$_{2.5}$	[126]
HKUST-1	HKUST-1/PAN	Direct electrospinning	CO$_2$	[225]

Fig. 6a, firstly, the PAN@ZIF-8 fiber precursor was prepared by electrospun, and then the PAN@ZIF-8 nanofiber membranes were calcined to acquire N-doped PCNFs. Finally, MoS$_2$ nanosheets were evenly assembled on the surface of PCNFs under hydrothermal conditions to obtain PCNF@MoS$_2$, whose microstructure is shown in Fig. 6b,

c. The resulted PCNF@MoS$_2$ hybrids were employed as anode materials for LIBs with large capacity, excellent cycle (Fig. 6d) and rate (Fig. 6e) properties. Additionally, Chen et al. demonstrated a valid multi-step route to prepare a hierarchical tubular structure composed of carbon nanotubes (CNTs) and Co$_3$O$_4$ hollow nanoparticles
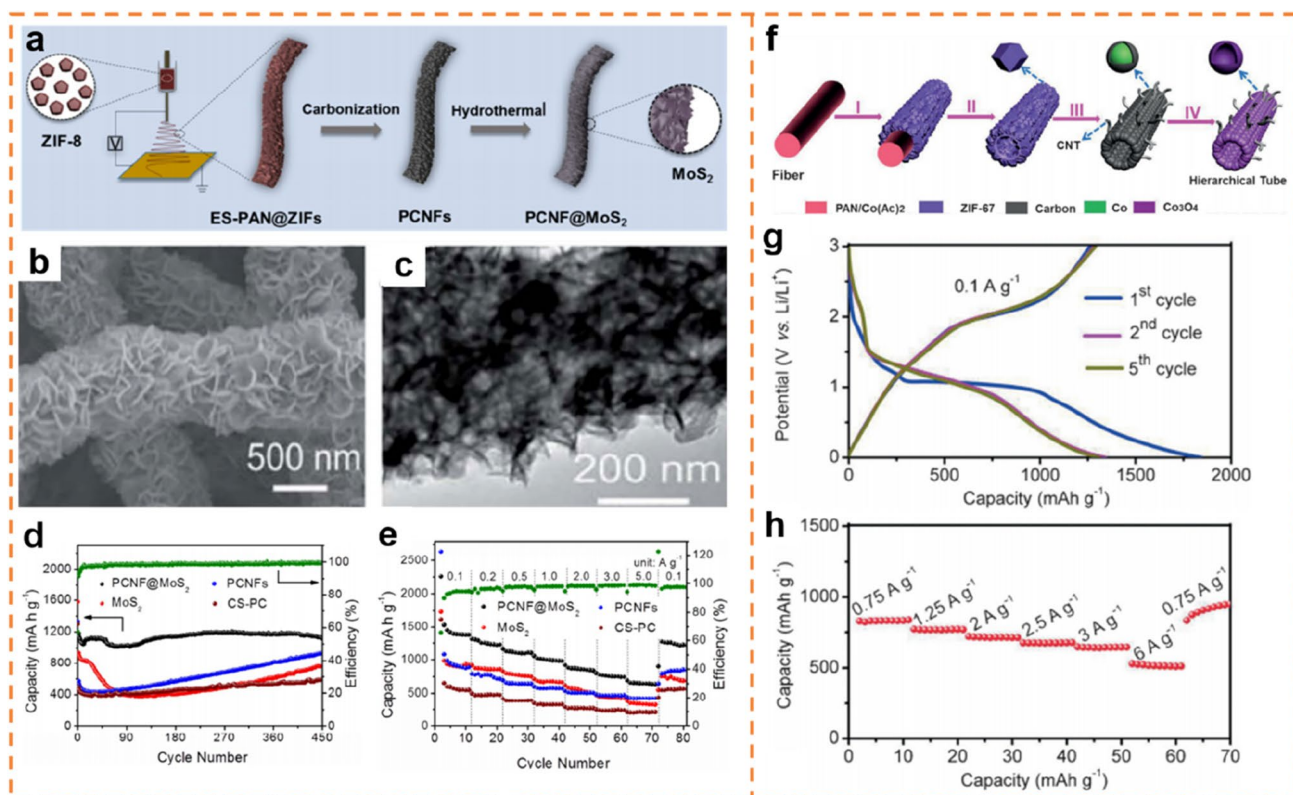
Fig. 6 **a** Schematic diagram for the fabrication process of the PCNF@MoS$_2$ fibers; **b** SEM and **c** TEM pictures of PCNF@MoS$_2$; **d** cycle property at 1.0 A·g^{-1}; **e** rate property at different current densities. Reproduced with permission from Ref [115]. Copyright 2019, Elsevier. **f** Preparation of the CNT/Co$_3$O$_4$ microtubes; Electrochemi- cal properties of the CNT/Co$_3$O$_4$ microtubes: **g** Charge–discharge voltage profiles at 0.1 A·g^{-1}; **h** rate performance at different current densities. Reproduced with permission from Ref [163]. Copyright 2016, Wiley–VCH

for lithium-ion batteries [163]. They prepared Co(AC)$_2$/ PAN fiber membranes by electrospun, and then soaked the fiber membranes into mIM solution to incorporate ZIF-67 crystals in the Co(AC)$_2$/PAN electrospun membranes by surface in situ growth. The resulting ZIF-67/PAN fibers could be converted into CNT/Co-carbon composites by a heat treatment in Ar/H$_2$. As illustrated in Fig. 6f, the CNT/ Co$_3$O$_4$ microtubes were obtained by further calcinating the composites. The structure of CNTs and Co$_3$O$_4$ hollow nanoparticles not only shortened the diffusion distance of lithium ions, but also provided enough contact for fast charge transfer between electrolytes and active materi- als. The CNTs could accelerate the rapid electron trans- fer and avert the accumulation of Co$_3$O$_4$ particles during cycling. Moreover, the derivative of ZIF-67 could relieve the volume expansion during electrochemical reactions. It is worth mentioning that the resulting CNT/Co$_3$O$_4$ com- posites delivered a high capacity of 1281 mAh·g^{-1} at 0.1 A·g^{-1} (Fig. 6g) with phenomenal rate (Fig. 6h) and excel- lent cycle performance as anode materials for LIBs.

Lithium-Sulfur Batteries

Lithium-sulfur batteries possess seductive theoretical spe- cific capacity [164–166]. However, the theoretical capacity is difficult to achieve due to the poor conductivity of sulfur elements [167]. Simultaneously, the polysulfides produced in the electrochemical reactions are prone to dissolve and move between negative and positive electrodes, resulting in the loss of active substances and the reduction of the perfor- mance of LSBs [168–170]. To improve the conductivity of electrode materials and suppress the shuttle of polysulfides, it is considered that the effective way is to develop electrode materials with high porosity, large specific surface area and homogeneous heteroatom doping as sulfur carriers [171]. The emerging MOF-derived porous carbon materials are regarded as potential candidates for LSBs [172–174].

Compared to other carbon nanofiber (CNF) materials, the developed ZIF-67-based CNFs as sulfur hosts can remark- ably improve the rate and the cycle performance of LSBs. Thanks to its exceptional structural stability and capacity

reversibility, sulfurized polyacrylonitrile (SPAN) possesses high value in the application of LSBs. Inspired by this, condensed and ultrathin SPAN membranes were designed and fabricated [175]. As visualized in Fig. 7a, ZIF-67 crystals were grown in situ on electrospinning fiber membranes composed of PAN and CNT. Then, surface-anchored CoS_2 nanoparticles were produced by a vulcanization process to acquire CoS_2-PAN-CNT composites as a cathode for LSBs. Impressively, the layer of CoS_2 nanoparticles on the surface of the fiber membranes efficiently suppressed membrane thickening and fiber expansion. Meanwhile, CoS_2 nanoparticles with high conductivity were conducive to accelerating the redox kinetics of sulfur conversion, so as to realize high-performance LSBs with greatly enhanced areal capacity. This research refreshes the current properties of SPAN batteries with the high capacitance (Fig. 7b), excellent cycle stability (Fig. 7c, d) and outstanding rate performance (Fig. 7e), revealing stupendous prospects for achieving flexible LSBs with large energy density. Additionally, the C/Co_9S_8@S hybrid carbon nanofibers as sulfur carriers were obtained by electrospinning and self-templating combined with solvothermal and calcination, as depicted in Fig. 7f [176]. The carbon case of the C/Co_9S_8 nanofibers derived from mIM in ZIF-67 could enhance the conductivity

of Co_9S_8, which assisted the transport of ion/electron and inhibited the departure of the sulfur to some extent. The hollow polyhedron structure of the C/Co_9S_8 hybrid fibers provided broad sulfur storage space and strong bonding for polysulfide. As a cathode for LSBs, the C/Co_9S_8–C@S hybrid fibers displayed an initial specific capacity of 1013.7 $mAh·g^{-1}$ at 0.1 C, exhibiting a capacity of 694.9 $mAh·g^{-1}$ after 150 cycles (Fig. 7g). Excitedly, the specific capacity reached 894.7 $mAh·g^{-1}$ at 1 C, and the capacity attenuation of each cycle was about 0.116% over 500 cycles (Fig. 7h).

Sodium-Ion Batteries

Sodium in sodium-ion batteries (SIBs) is abundant and inexpensive on Earth [177–179]. Unfortunately, the electrode materials used in LIBs cannot meet the ideal reversible capacity and cycle performance of SIBs because the radius of sodium ions (1.02 Å) is larger than that of lithium ions (0.76 Å) [180–183]. Therefore, the structural stability and reaction kinetics of SIBs are affected [184, 185]. Fortunately, the one-dimensional carbon electrospun nanofibers derived from MOF with a high specific surface area have good conductivity and structural stability, which could not only produce some spacious channels for the transmission of
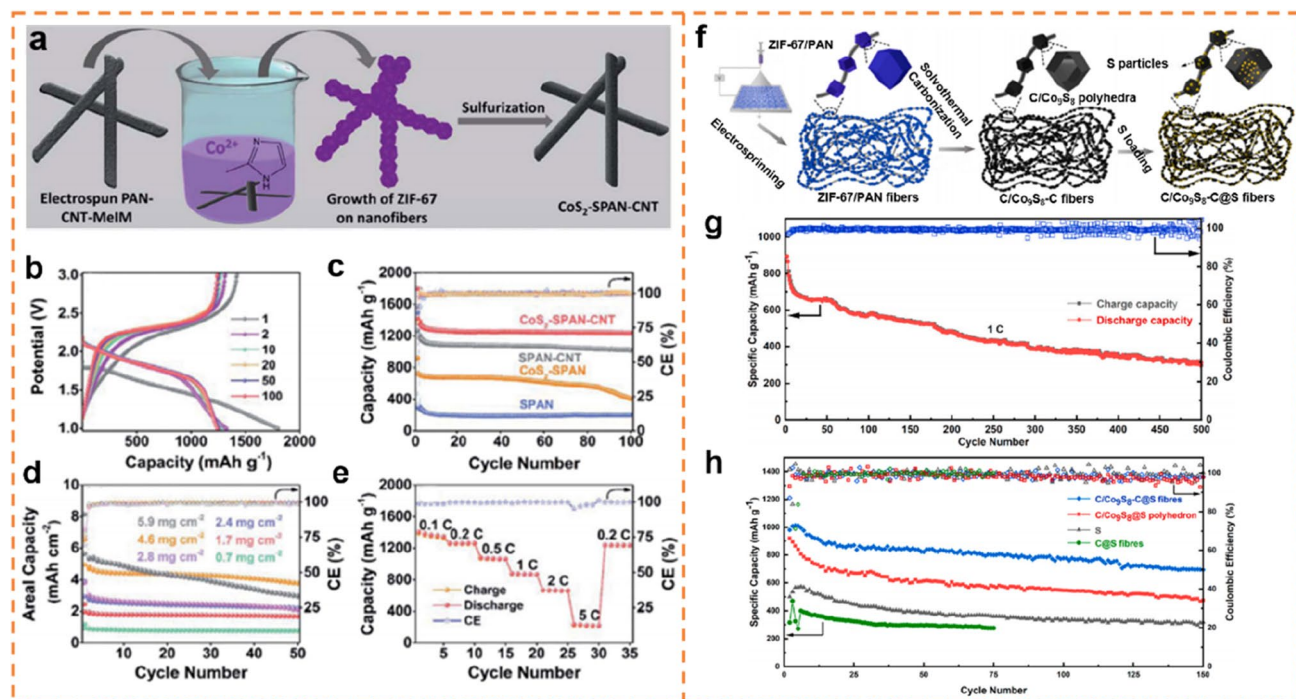

Fig. 7 **a** Schematic diagram of the fabrication of the CoS_2–SPAN–CNT electrode; **b** charge/discharge profiles at a sulfur loading of 2.4 mg·cm^{-2} at 0.2 C; **c** cycle properties of the CoS_2–SPAN–CNT and control samples at 0.2 C; **d** cycle properties of CoS_2–SPAN–CNT with areal sulfur loadings at 0.2 C; **e** rate capability from 0.1 to 5 C. Reproduced with permission from Ref [175]. Copyright 2020, the

Royal Society of Chemistry. **f** Schematic diagram of the fabrication route for C/Co_9S_8–C@S nanofiber; **g** cycle properties and coulombic efficiency of the C/Co_9S_8–C@S nanofibers at 1 C; **h** cycle properties and coulombic efficiency of C/Co_9S_8–C@S nanofibers, C/Co_9S_8@S polyhedron, C@S nanofibers and the sulfur cathode at 0.1 C. Reproduced with permission from Ref [176]. Copyright 2021, Elsevier

ion and electron in SIBs, but also relieve the volume expansion during the cycle of SIBs [186–190]. Furthermore, entangling one-dimensional carbon nanofibers into a three-dimensional conductive matrix implanted with heterogeneous nanoparticles can satisfy faster diffusion kinetics and shorten the diffusion distance of ions [191, 192].

Combining simple electrospinning and subsequent annealing treatments, a one-dimensional N-doped PCNF anchoring amorphous and graphite carbon-encapsulated CoS_2 particles (AGC-CoS_2@NCNFs) was successfully fabricated as an anode for SIBs. It exhibited superior electrochemical performance [193]. The fabrication process and microstructure of the composite are displayed in Fig. 8a–c. Remarkably, the rationally designed composite possessed improved Na-storage performance. It is worth mentioning that the electrode material shows outstanding rate properties at different current densities (Fig. 8d), a large specific capacity of 876 mAh·g^{-1} at 100 mA·g^{-1} and an exceptional cycle performance of 148 mAh·g^{-1} at 3.2 A·g^{-1} over 1000 cycles (Fig. 8e). The research indicated

that the enhancement of electrochemical performance was attributed to the one-dimensional N-doped PCNF structure and the graphitic carbon covering, which could cleverly restrain aggregation of CoS_2 particles and alleviate the volume changes in electrochemical reactions to some extent. Additionally, a three-dimensional Fe_7S_8 particles/N-doped carbon nanofibers (Fe_7S_8/N-CNFs) composite was designed and prepared via facile electrospinning and subsequent calcination treatment by Wang et al. [194]. The preparation process of Fe_7S_8/N-CNFs is illustrated in Fig. 8f. As depicted in Fig. 8 g and h, Fe_7S_8 particles were encapsulated in the three-dimensional interconnected Fe_7S_8/N-CNFs with a unique structure. When the Fe_7S_8/N-CNFs composite was employed as a negative electrode for SIBs, a high capacity of 649.9 mAh·g^{-1} was retained after 100 cycles at 0.2 A·g^{-1} (Fig. 8i) and excellent cycle stability was realized (Fig. 8j). The acquired composite exhibited the following advantages: (I) Fe_7S_8 particles originated from MIL-88A(Fe) could reduce the diffusion distance of sodium ions; (II) the unique three-dimensional structure enhanced the conductivity and
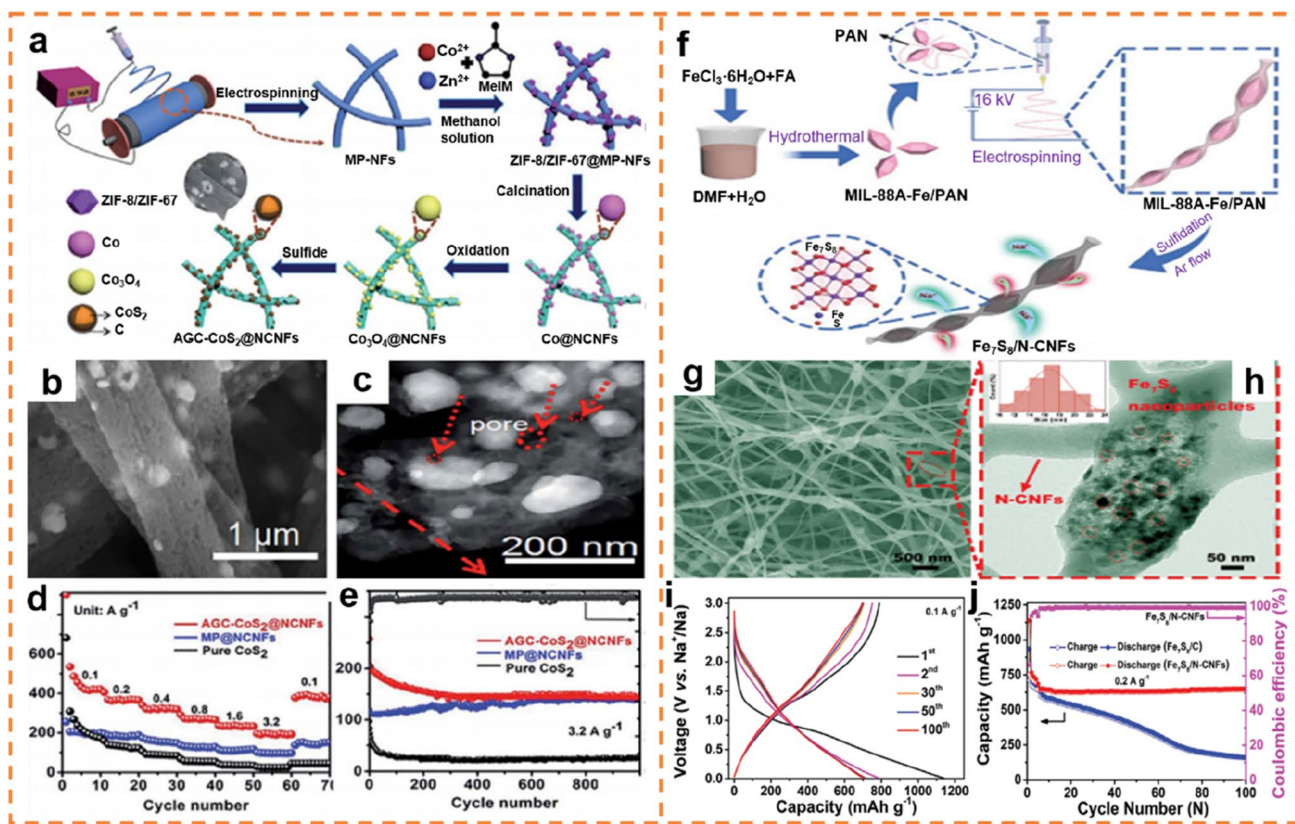

Fig. 8 a Schematic illustration of the fabrication of AGC-CoS_2@NCNFs; b SEM and c TEM images of AGC-CoS_2@NCNFs; d rate performance of AGC-CoS_2@NCNFs; e long-term cycle performance at a 3.2 A·g^{-1} current density. Reproduced with permission from Ref [193]. Copyright 2020, Elsevier. f Schematic diagram of the synthetic process of Fe_7S_8/N-CNFs; g FESEM picture of Fe_7S_8/N-CNFs; h HRTEM picture and nanoparticle size distribution (the inset) of Fe_7S_8/N-CNFs; i charge/discharge curves of the Fe_7S_8/N-CNFs electrode for the first, second, 30th, 50th and 100th cycles at 0.1 A·g^{-1}; j cycle performance and coulombic efficiency of the Fe_7S_8/N-CNFs electrode at 0.2 A·g^{-1}. Reproduced with permission from ref [194]. Copyright 2021, Wiley–VCH

alleviated the volume changes and self-aggregation of Fe_7S_8 nanoparticles; and (III) abundant active sites for sodium ions adsorption and paths for electrolyte diffusion were provided. These researches shed light on the development of anode materials for SIBs with superior electrochemical performance.

Water Treatment

Presently, shortage of drinking water and wastewater pollution have given rise to strong demand for water purification via cost-efficient and energy-savings ways [195]. Unfortunately, conventional single filtration and adsorption technologies are unable to simultaneously remove pollutants of different sizes from wastewater, especially heavy metals, dyes and bacteria [67, 196, 197]. Consequently, the development of energy-savings, cost-effective and advanced wastewater purification materials has been widely regarded as the most critical research segment in this field. Emerging MOF materials can adsorb pollutants from wastewater owing to their large surface area, high porosity and easy modification. However, they are powder materials that are easy to agglomerate, resulting in a decrease in adsorption capacity. It is difficult to efficiently recover these powder materials from wastewater, which is easy to cause secondary pollution [198, 199]. Recently, numerous researches on MOF-based nanofibrous membranes have been implemented for the applications of wastewater treatment, indicating that MOF-based nanofibrous membranes possess an extraordinary potential in removing pollutants from wastewater [200, 201]. This section systematically summarizes the application of MOF-based nanofiber membranes for the removal of heavy metals and dyes from wastewater.

Heavy Metal Ions

The residual heavy metals in water pose a severe threat to the life and health of human beings [202–204]. It is imperative to effectively remove them from wastewater. In an excellent research, modified-MOF (MOF-808-EDTA) nanoparticles loaded PAN membranes were designed and fabricated through solvothermal treatment and electrospun to simultaneously adsorb heavy metal ions and separate oil–water [205]. The preparation process of MOF-808@PAN electrospun fiber membranes and the mechanisms of heavy metal ions adsorption and oil-in-water emulsions separation are revealed in Fig. 9a. Interestingly, the composite membranes exhibited superoleophobicity in water and could effectively separate oil-in-water emulsions (Fig. 9b). Meanwhile, the powerful adsorption capacity of MOF-808-EDTA allowed the nanofiber membranes to capture heavy metal ions (Pd^{2+}, Cu^{2+}, Cr^{2+} and Cr^{3+}) at different concentrations within a short period (Fig. 9c), indicating outstanding adsorption capacity for removing heavy metal ions from wastewater. It is worth mentioning that the membranes also exhibited outstanding corrosion resistance and recyclability. The ZIF-67-based "pearl-necklace-like" hybrid fiber membranes were synthesized by in situ growth on the surface of mIM/cellulose acetate (mIM/CA) electrospinning nanofibers, as illustrated in Fig. 9d [206]. When ZIF-67 crystals were approximately saturated, the surface area of the integrated composite nanofiber membranes was much higher (463.1 $m^2 \cdot g^{-1}$), which was dozens of times that of the primitive mIM/CA electrospinning fibers (6.9 $m^2 \cdot g^{-1}$). Attractively, the composite nanofiber membranes exhibited a remarkable adsorption capacity of Cr^{6+} (14.5 $mg \cdot g^{-1}$) and Cu^{2+} (18.9 $mg \cdot g^{-1}$), as displayed in Fig. 9 e and f. Moreover, the adsorption mechanisms of the composite membranes were analyzed. It was concluded that the ions exchange and electrostatic adsorption made a contribution to the excellent adsorption capacity for Cr^{6+} and Cu^{2+}. Additionally, the appearance of Cr^{3+} ions indicated that the Cr^{6+} ions partially conversed to Cr^{3+} during the adsorption. This work demonstrates that the composite membranes were potential environmental materials for the removal of heavy metals from wastewater.

Dyes

The dyes released into the water are toxic and even carcinogenic. They are difficult to degrade spontaneously, which cause great harm to human health and the green environment [207, 208]. To solve the problem of dyes pollution, a variety of strategies have been performed to capture organic dyes from wastewater [209–211]. The bio-MOF/PAN nanofibrous filter was cleverly prepared by co-electrospun of bio-MOF-1 $(Zn_8(Ad)_4(BPDC)_6O \cdot 2(NH_2(CH_3)_2)^+, 8DMF, 11H_2O)$ with an anionic skeleton and PAN for selective separation and capture of cationic dyes from an aqueous solution, as illustrated in Fig. 9g [212]. Due to the existence of the free $NH_2(CH_3)^{2+}$ cations from the channels of bio-MOF-1 and the nucleophilic groups from PAN, bio-MOFs-1 and PAN possessed outstanding adsorption capacity for cationic dyes. Owing to the synergistic interaction of PAN and bio-MOF-1, the bio-MOF/PAN filter displayed a quick adsorption rate for methylene blue (MB^+) (Fig. 9h) and achieved the rapid capture of MB^+ from the solution of mixed dyes. It is worth mentioning that the bio-MOF/PAN filter could be efficiently regenerated via ion exchange. Remarkably, it still maintained stable adsorption values for MB^+ after the five cycles of filtration-regeneration (Fig. 9i), manifesting that the bio-MOF/PAN filter had the ability to retain a long service life. Additionally, Dai et al. proposed an experimental scheme to coat ZIF-8@GO on the surface of polylactic acid (PLA) electrospinning
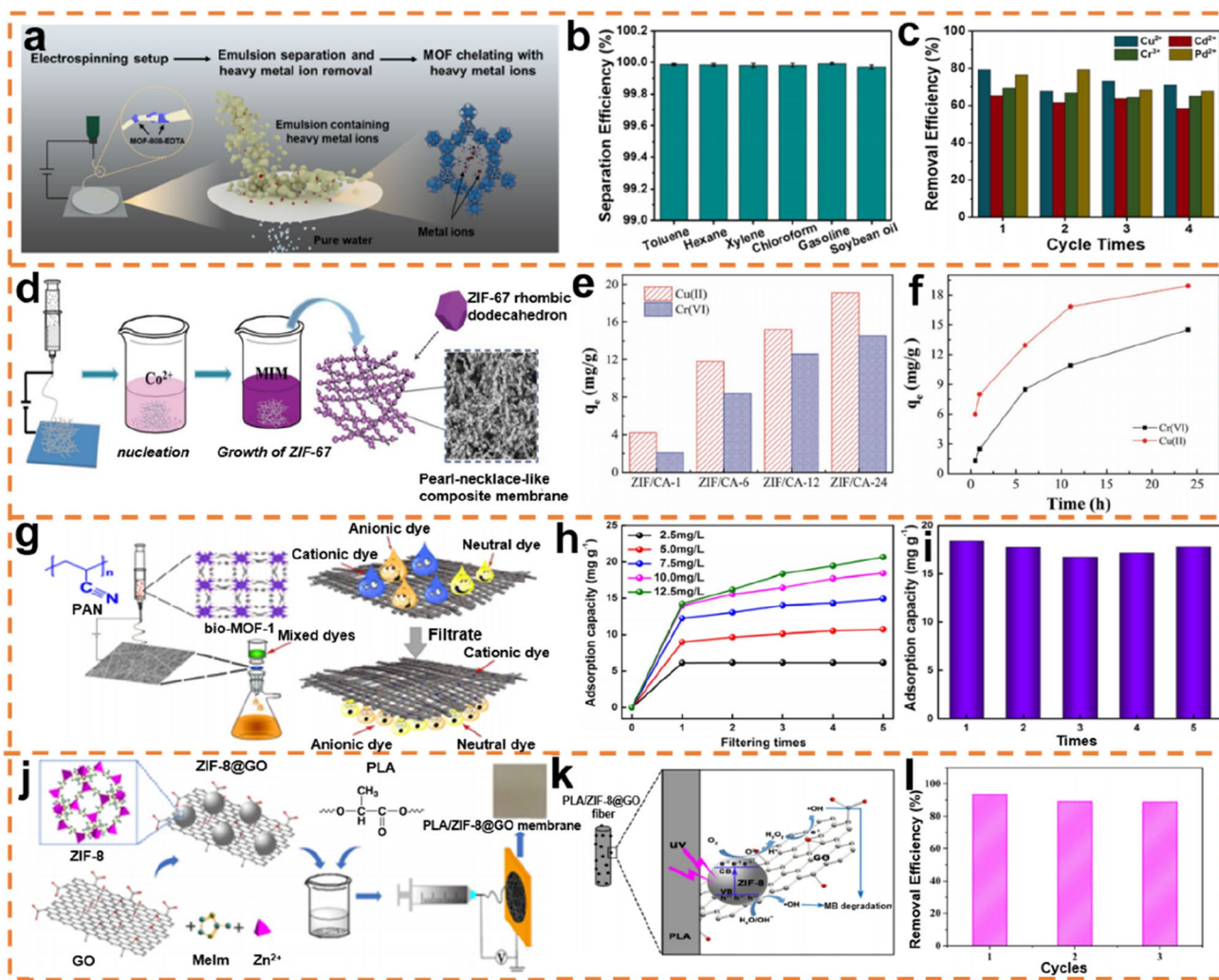
Fig. 9 **a** Preparation of the MOF-808@PAN nanofiber membranes and mechanisms of heavy metal capture and oil-in-water emulsions separation; **b** separation efficiency of different oil-in-water emulsions; **c** cycle test of the adsorption capacity of the MOF-808@PAN nanofiber membranes for different heavy metal. Reproduced with permission from Ref [205]. Copyright 2020, American Chemical Society. **d** Schematic diagram of the fabrication of pearl-necklace-like composite fiber membranes; **e** adsorption capacity of all samples for Cr^{6+} and Cu^{2+}; **f** effect of contact time on the adsorption of Cr^{6+} and Cu^{2+} on the ZIF/CA-24 (experimental condition: at room temperature, pH ≈ 6.5, without stirring). Reproduced with permission from Ref [206]. Copyright 2018, Wiley–VCH. **g** Preparation of bio-MOF/PAN membrane and its adsorption of cationic dyes; **h** adsorption capacity of bio-MOF/PAN filter for MB^+ with different original concentrations; **i** adsorption capacity of bio-MOF/PAN filter for MB^+ in five cycles. Reproduced with permission from Ref [212]. Copyright 2020, Elsevier. **j** Fabrication Process of the PLA/ZIF-8@GO composite nanofiber membranes; **k** mechanisms of photocatalytic degradation of MB on PLA/ZIF-8@GO nanofibers; **l** removal efficiency of MB on PLA/ZIF-8@GO nanofibers with three cycles. Reproduced with permission from Ref [213]. Copyright 2018, American Chemical Society

nanofiber membranes via in situ growth for photocatalytic degradation and adsorption MB [213]. As shown in Fig. 9j, k, the fabrication process of the ZIF-8@GO/PLA fiber membranes and the mechanisms of photocatalytic degradation are revealed, respectively. During the reaction, PLA acted as an adsorbent and catalyst carrier, and ZIF-8 produced holes and photogenerated electrons under illumination, which facilitates a series of reactions. Simultaneously, GO served as a paralysis of electron–hole pairs recombination, which could enhance the performance of the hybrid fiber membranes. The results demonstrated that the degradable ZIF-8@GO/PLA electrospun nanofiber membranes delivered higher tensile strength than pure PLA. Satisfactorily, the composite nanofiber membranes exhibited excellent MB removal efficiency by photocatalytic degradation and adsorption. In the case of a shallow ZIF-8@GO concentration (0.06 mg·mL^{-1}), the removal efficiency of MB could still reach over 90% after three cycles (Fig. 9l).

Air Pollutant Filtration

With the development of worldwide industrialization, atmospheric pollutants in the form of toxic gases and delicate particulate matter (PM) have become a severe worldwide environmental issue [214, 215]. Past studies have demonstrated that adsorbents such as zeolites, activated carbon, resins, biomass and metal oxides can capture these pollutants from the atmosphere [210, 216, 217]. Unfortunately, the high regeneration cost and limited adsorption capacity of these traditional materials have forced researchers to develop novel materials and technologies to remove air pollutants [218]. Researchers found that the nanofibers prepared by electrospinning possess the advantages of controllable pore size, large specific surface area and high air permeability [94]. Furthermore, the composites fabricated by loading MOF crystals on nanofibers have significantly improved removal ability, so they are considered candidates for rapid and effective capture of pollutants from the air [219].

Toxic Gases

Sulfur dioxide (SO_2) and ozone (O_3), the primary pollutants in the air, pose a serious threat to the biological system and human health. Fortunately, MOF-based electrospun nanofibers can effectively capture SO_2 and O_3 from the air. For example, MIL-53(Al)–NH_2/PAN hybrid fiber membranes prepared by in situ growth of MIL-53(Al)–NH_2 crystals onto the surface of PAN polymer nanofibers via electrospinning

technology and subsequent hydrothermal treatment exhibited outstanding adsorption capacity for air pollutants, especially PM, sulfur trioxide (SO_3) and O_3 [220]. The preparation process is shown in Fig. 10a. Remarkably, the PM removal efficiency of the obtained composite nanofiber membranes could reach 99.99%. More interestingly, the MIL-53(Al)–NH_2/PAN composite fiber membranes could selectively and efficiently remove SO_2 and O_3 pollutants without being affected by carbon dioxide (CO_2), oxygen (O_2) and other gases. The composite nanofiber membranes could not only reduce the SO_2 concentration from 7300 to 40 ppb (Fig. 10b), but also rapidly drop the O_3 concentration from 3000 to 7 ppb (Fig. 10c), which is far lower than the national air quality standard (81 ppb). This work indicated that the great potential of the composite membranes prepared by simple and cheap electrospinning technology as candidate materials for air purification and environmental protection.

Particulate Matter

PM with small size can enter the respiratory system through the respiratory tract, which causes respiratory diseases, such as upper respiratory tract infection, bronchial asthma, bronchitis, pharyngitis, pneumonia. The MOF-based electrospun nanofibers can not only remove SO_2 and O_3 from the air, but also effectively capture PM. As the first work to explore the interaction between MOF-based nanofibrous membranes and PM, Zhang et al. designed four kinds of MOF/polymer nanofibrous membranes (UiO-66-NH_2/PAN, ZIF-8/PAN,
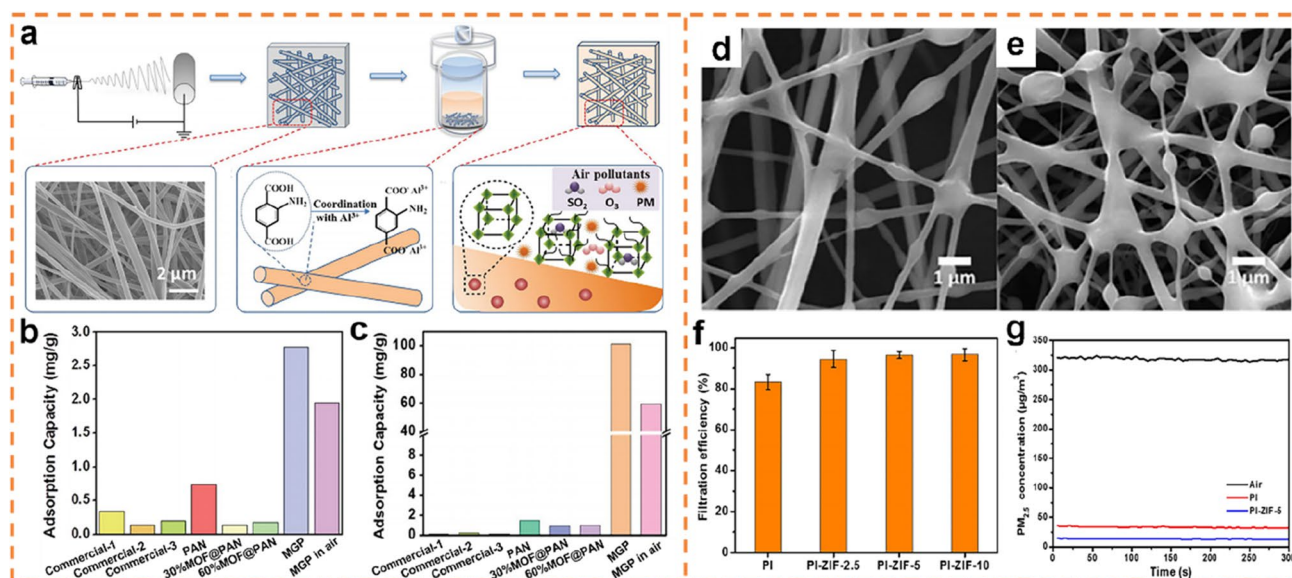

Fig. 10 a The fabrication and adsorption processes of MOF-based nanofiber membranes; **b** SO_2 removal capacity of the different fiber membranes; **c** O_3 removal capacity of the different fiber membranes. Reproduced with permission from Ref [220]. Copyright 2019, the Royal Society of Chemistry. SEM images of **d** PI membranes and **e** ZIF-8/PI membranes; **f** $PM_{2.5}$ removal efficiency of different membranes; **g** the concentration of $PM_{2.5}$ captured by different membranes in harsh conditions. Reproduced with permission from Ref [126]. Copyright 2019, American Chemical Society

MOF-199/PAN and Mg-MOF-74/PAN) with loadings up to 60% [221]. The performance of these four MOF/polymer nanofiber filters was investigated in an actual smog environment ($PM_{10}=720$ μg·m^{-3}, $PM_{2.5}=350$ μg·m^{-3}). The results displayed that ZIF-8/PAN exhibited the strongest capacity to remove PM ($89.67 \pm 1.33\%$ for PM_{10}, $88.33 \pm 1.52\%$ for $PM_{2.5}$), and the performance did not decrease obviously after 48 h of continuous exposure. The excellent PM removal capacity of ZIF-8/PAN was attributed to the highest zeta potential value of ZIF-8. Interestingly, these fiber filters could selectively capture SO_2 when exposed to SO_2/N_2. Commendably, their hierarchical nanostructures allowed the permeation of fresh air at high gas flow rates (pressure drop < 20 Pa). Additionally, a strategy combining electrospinning was designed to prepare ZIF-8/PI composite nanofiber membranes with different loadings of ZIF-8 crystals [126]. SEM characterization demonstrated that the hybrid fiber membranes obtained by introducing ZIF-8 nanoparticles displayed a rougher surface than the pure PI membranes (Fig. 10d, e). As shown in Fig. 10f, compared with the pure PI membranes, the ZIF-8/PI composite membranes exhibited a higher removal efficiency for $PM_{2.5}$, which was attributed to the larger specific surface area of the composite membranes and the excellent properties of ZIF-8, such as exceptional chemical and thermal stability (up to 300 °C). Interestingly, ZIF-8/PI composite nanofiber membranes with ZIF-8 loading of 10% exhibited the highest $PM_{2.5}$ removal rate ($96.6 \pm 2.9\%$). Additionally, the composite membranes could efficiently capture $PM_{2.5}$ in a short time, even under harsh conditions, which is quite remarkable (Fig. 10g).

Gas Storage and Separation

The increase of population and the development of global industrialization have led to the increasing CO_2 emission, which poses a serious threat to human health and the ecological environment [222]. In recent years, MOFs have received increasing attention owing to their large specific surface area, high porosity, tunable pore size and flexible framework structures [223]. Unfortunately, a single MOF material may suffer from blockage of pipelines and difficulty in recycling in practical gas storage and separation work [224]. To address these issues, the researchers constructed MOF materials with porous structures into nanofiber membranes by electrospinning to introduce more efficient adsorption sites. The resulting MOF-based nanofibrous membranes play a major role in scaling up practical applications for gas storage and separation.

It is found that the size, loading amount, morphology and specific surface area of MOF crystals supported on the fibrous membranes greatly affect the properties of MOF/polymer nanofiber membranes. For example, the flexible and self-supporting HKUST-1/PAN nanofiber membranes with MOF particles loading up to 82% prepared by electrospinning can efficiently and selectively adsorb CO_2 [225]. This is the work with the highest MOF loading rate at present. Surprisingly, the designed HKUST-1/PAN nanofibrous membranes exhibited outstanding CO_2 adsorption capacity (3.9 mmol·g^{-1}) and excellent CO_2/N_2 selectivity. It is worth mentioning that the results of 100 adsorption–desorption experiments showed that the CO_2 adsorption capacity hardly changed and remained at 95% (3.7 mmol·g^{-1}) of the initial value, revealing the potential of stable recoverability and excellent practical value of HKUST-1/PAN nanofiber membranes. The abundant CO_2 adsorption sites on the nanofibrous membranes are mainly located in the open metal sites. In addition, the designed HKUST-1/PAN nanofibrous membranes possessed ultra-high specific surface area, suitable pore size and porosity, which made a significant contribution to the selective separation of CO_2/N_2. This work provides a low-cost and scalable production route to convert MOF crystals into flexible and self-supporting nanofibrous membranes, laying the cornerstone for better post-combustion CO_2 capture.

Conclusion and Perspectives

In recent years, MOFs have received increasing attention owing to their large specific surface area, high porosity, tunable pore size and flexible framework structures. However, due to the limitations of MOFs, a single MOF material cannot well satisfy the needs of practical applications. Fortunately, a series of MOF composites and derivatives have been gradually discovered and studied. Among them, MOF/polymer nanofibers fabricated by electrospinning have been intensively reported. The resulting composites not only overcome the limitations of single MOF materials, but also realize co-spinning of multiple materials, significantly improving the diversity of nanofibers and broadening the applications of MOF/polymer nanofibers. Based on this, researchers have conducted a large number of reports on them. This review systematically summarizes the two main routes (direct electrospinning and surface in situ growth) for the preparation of MOF/polymer nanofiber membranes by electrospun combined with other methods, such as hydrothermal and solvothermal reactions. Both routes can successfully prepare nanofibrous membranes with high specific surface area, large porosity and superior air permeability. Next, the applications of MOF/polymer nanofiber membranes prepared by these two routes in lithium-ion batteries, lithium-sulfur batteries, sodium-ion batteries and environmental protection are discussed. Although great progress has been achieved in the applications of MOF-based nanofiber membranes, there are still various inevitable challenges and

problems in future research, as shown in the following six points.

(1) Although thousands of MOF nanoparticles have been successfully prepared, the MOFs developed as precursors are limited to traditional structures, such as MIL and ZIF series. Consequently, MOF-based nanomaterials generally have similar structures and morphologies, which is not conducive to realizing the structural diversity, but also affects the further improvement of the performance of related materials. Hence, it is necessary to develop a wide variety of MOFs as precursors of MOF-based nanomaterials to exploit the greater potential of materials. Meanwhile, the development of these novel MOFs is beneficial to expanding the raw material sources for MOF/polymer systems, paving the way for obtaining higher-performance MOF/polymer nanofibers.

(2) Considering the enrichment of nanofiber types and the development of more potential MOF/polymer nanofiber materials, more polymer materials can be investigated to develop diverse MOF/polymer systems. However, these polymers should be guaranteed to withstand harsh MOF synthesis and decoration conditions, such as aggressive solvents and temperatures.

(3) Post-processing technology has been widely used in the processing of traditional nonwoven fibers in the textile industry. Future research can focus on exploring the synergistic mechanism of MOF crystals and polymer electrospun nanofibers. Then, appropriate post-processing technology is adopted to improve the performance of MOF/polymer nanofibers to expand its practical applications.

(4) In recent years, the types and structures of MOF/polymer nanofibers have gradually increased. Still, there are few theoretical studies to illustrate the relationship between structure and performance, which is not conducive to achieving controllability of material composition and structure. For instance, porous carbon nanomaterials derived from MOFs obtained by metal ion removal and carbonization treatments may exhibit large structural uncertainties. Because MOF/polymer nanofibers are a relatively new architecture, more theoretical studies on the structural evolution of fibers during the post-processing are required to satisfy the practical needs.

(5) Although MOF/polymer nanofibers possess obvious advantages in structure and performance, there are also some disadvantages that cannot be ignored. Unfortunately, no commercial products of MOF/polymer fibers have been reported so far. The high cost of semifinished materials and the complicated preparation process may be the reasons that restrain the large-scale production of the composite in commerce. Some traditional MOFs can be synthesized with cheap metal ions and organic ligands, but low yield usually leads to high cost. Consequently, developing inexpensive ligands with guaranteed high yield is the direction for the further development of MOF/polymer nanofibers. Additionally, improving the related equipment and facilities for the production of MOF/polymer nanofibers is also a significant breakthrough. These improvements are expected to allow MOF-based nanofibers to enter the market of high commercial value for the first time. For example, MOF-based nanofibers can be used to capture contaminants in water.

(6) MOF/polymer nanofiber membranes have been widely used in energy storage and environmental protection. However, the problems of poor stability, high cost and poor regeneration ability in practical applications limit the further development of fiber membranes. All research results need to be scaled from laboratory to large-scale production and application. Therefore, it is a great challenge and opportunity to design MOF/polymer nanofiber membranes that are both economical and environmentally friendly for commercial applications. In addition, appropriate post-treatment technologies can be applied to the modification of MOF/polymer nanofiber membranes to enhance their stability and feasibility in practical applications.

MOF/polymer nanofiber membranes have been widely used in energy storage and environmental protection. However, the development of MOF/polymer electrospun fiber membranes with fewer defects, higher chemical stability and lower cost brings great challenges and opportunities for future research. In conclusion, MOF-based nanofibers hold the promise of playing a central role in energy storage and environmental protection. Researchers can conduct more in-depth research on MOF-based nanofibers, and ultimately promote the better applications of MOF-based nanofiber membranes in energy storage and environmental protection.

Declarations

Conflict of Interest The authors declare that they have no conflict of interest.

References

1. Chu S, Majumdar A. Opportunities and challenges for a sustainable energy future. *Nature* **2012**;*488*:294–303.

2. Hung TH, Deng X, Lyu Q, Lin LC, Kang DY. Coulombic effect on permeation of CO_2 in metal-organic framework membranes. *J Memb Sci* **2021**;*639*:119742.

3. Heald CL, Spracklen DV. Land use change impacts on air quality and climate. *Chem Rev* **2015**;*115*:4476–96.

4. Zhou L, Tufail MK, Liao Y, Ahmad N, Yu P, Song T, et al. Tailored carrier transport path by interpenetrating networks in cathode composite for high performance all-solid-state Li-SeS$_2$ batteries. *Adv Fiber Mater* **2022**;*4*:487–502.

5. Cheng H, Yan C, Orenstein R, Dirican M, Wei S, Subjalearndee N, et al. Polyacrylonitrile nanofiber-reinforced flexible single-ion conducting polymer electrolyte for high-performance, room-temperature all-solid-state Li-metal batteries. *Adv Fiber Mater* **2022**;*4*:532–46.

6. Wang S, Xu Q, Sun H. Functionalization of fiber devices: materials, preparations and applications. *Adv Fiber Mater* **2022**;*4*:324–41.

7. Shakoor MB, Nawaz R, Hussain F, Raza M, Ali S, Rizwan M, et al. Human health implications, risk assessment and remediation of As-contaminated water: a critical review. *Sci Total Environ* **2017**;*601–602*:756–69.

8. Yang Y, Ok YS, Kim KH, Kwon EE, Tsang YF. Occurrences and removal of pharmaceuticals and personal care products (PPCPs) in drinking water and water/sewage treatment plants: a review. *Sci Total Environ* **2017**;*596–597*:303–20.

9. Sharma VK, Feng M. Water depollution using metal-organic frameworks-catalyzed advanced oxidation processes: a review. *J Hazard Mater* **2019**;*372*:3–16.

10. Liu X, Shan Y, Zhang S, Kong Q, Pang H. Application of metal organic framework in wastewater treatment. *Green Energy Environ* **2022**. https://doi.org/10.1016/j.gee.2022.03.005 .

11. Jun BM, Al-Hamadani YAJ, Son A, Park CM, Jang M, Jang A, et al. Applications of metal-organic framework based membranes in water purification: a review. *Sep Purif Technol* **2020**;*247*:116947.

12. Yu S, Pang H, Huang S, Tang H, Wang S, Qiu M, et al. Recent advances in metal-organic framework membranes for water treatment: a review. *Sci Total Environ* **2021**;*800*:149662.

13. Li W, Liu YY, Bai Y, Wang J, Pang H. Anchoring ZIF-67 particles on amidoximerized polyacrylonitrile fibers for radionuclide sequestration in wastewater and seawater. *J Hazard Mater* **2020**;*395*:122692.

14. Lv K, Fichter S, Gu M, März J, Schmidt M. An updated status and trends in actinide metal-organic frameworks (An-MOFs): from synthesis to application. *Coord Chem Rev* **2021**;*446*:214011.

15. Zhou D, Zhao L, Li B. Recent progress in solution assembly of 2D materials for wearable energy storage applications. *J Energy Chem* **2021**;*62*:27–42.

16. Burdyny T, Smith WA. CO_2 reduction on gas-diffusion electrodes and why catalytic performance must be assessed at commercially-relevant conditions. *Energy Environ Sci* **2019**;*12*:1442–53.

17. Wang Z, Roffey A, Losantos R, Lennartson A, Jevric M, Petersen AU, et al. Macroscopic heat release in a molecular solar thermal energy storage system. *Energy Environ Sci* **2019**;*12*:187–93.

18. Chen Y, Wu H, Xiao Q, Lv D, Li F, Li Z, et al. Rapid room temperature conversion of hydroxy double salt to MOF-505 for CO_2 capture. *CrystEngComm* **2019**;*21*:165–71.

19. Bennett TD, Cheetham AK. Amorphous metal−organic frameworks. *Acc Chem Res* **2014**;*47*:1555–62.

20. Zhang Y, Su Q, Xu W, Cao G, Wang Y, Pan A, et al. A confined replacement synthesis of bismuth nanodots in MOF derived carbon arrays as binder-free anodes for sodium-ion batteries. *Adv Sci* **2019**;*6*:1900162.

21. Morozan A, Jaouen F. Metal organic frameworks for electrochemical applications. *Energy Environ Sci* **2012**;*5*:9269–90.

22. Liu P, Redekop E, Gao X, Liu WC, Olsbye U, Somorjai GA. Oligomerization of light olefins catalyzed by Brønsted-acidic metal-organic framework-808. *J Am Chem Soc* **2019**;*141*:11557–64.

23. Zhu S, Zhao N, Li J, Deng X, Sha J, He C. Hard-template synthesis of three-dimensional interconnected carbon networks: rational design, hybridization and energy-related applications. *Nano Today* **2019**;*29*:100796.

24. Arbulu RC, Jiang YB, Peterson EJ, Qin Y. Metal-organic framework (MOF) nanorods, nanotubes, and nanowires. *Angew Chem Int Ed* **2018**;*57*:5813–7.

25. Liu W, Yin R, Xu X, Zhang L, Shi W, Cao X. Structural engineering of low-dimensional metal-organic frameworks: synthesis, properties, and applications. *Adv Sci* **2019**;*6*:1802373.

26. Ren Q, Wang H, Lu XF, Tong YX, Li GR. Recent progress on MOF-derived heteroatom-doped carbon-based electrocatalysts for oxygen reduction reaction. *Adv Sci* **2018**;*5*:1700515.

27. Rani P, Srivastava R. Exploring the dicationic gemini surfactant for the generation of mesopores: a step towards the construction of a hierarchical metal-organic framework. *Inorg Chem Front* **2018**;*5*:2856–67.

28. Dhakshinamoorthy A, Li Z, Garcia H. Catalysis and photocatalysis by metal organic frameworks. *Chem Soc Rev* **2018**;*47*:8134–72.

29. Zhang C, Shen L, Shen J, Liu F, Chen G, Tao R, et al. Anion-sorbent composite separators for high-rate lithium-ion batteries. *Adv Mater* **2019**;*31*:1808338.

30. Wang Y, Feng L, Pang J, Li J, Huang N, Day GS, et al. Photosensitizer-anchored 2D MOF nanosheets as highly stable and accessible catalysts toward artemisinin production. *Adv Sci* **2019**;*6*:1802059.

31. Cao S, Chen T, Zheng S, Bai Y, Pang H. High-performance capacitive deionization and killing microorganism in surface-water by ZIF-9 derived carbon composites. *Small Methods* **2021**;*5*:2101070.

32. Ma Z, Zheng R, Liu Y, Ying Y, Shi W. Carbon nanotubes interpenetrating MOFs-derived Co-Ni-S composite spheres with interconnected architecture for high performance hybrid supercapacitor. *J Colloid Interface Sci* **2021**;*602*:627–35.

33. Aslam MK, Ahmad Shah SS, Javed MS, Li S, Hussain S, Hu B, et al. FeCo-Nx encapsulated in 3D interconnected N-doped carbon nanotubes for ultra-high performance lithium-ion batteries and flexible solid-state symmetric supercapacitors. *J Electroanal Chem* **2019**;*855*:113615.

34. Dai S, Han F, Tang J, Tang W. MOF-derived Co_3O_4 nanosheets rich in oxygen vacancies for efficient all-solid-state symmetric supercapacitors. *Electrochim Acta* **2019**;*328*:135103.

35. Ngyuen DK, Schepisi IM, Amir FZ. Extraordinary cycling stability of $Ni_3(HITP)_2$ supercapacitors fabricated by electrophoretic deposition: cycling at 100,000 cycles. *Chem Eng J* **2019**;*378*:122150.

36. Peng Y, Bai Y, Liu C, Cao S, Kong Q, Pang H. Applications of metal–organic framework-derived N, P, S doped materials in electrochemical energy conversion and storage. *Coord Chem Rev* **2022**;*466*:214602.

37. Senthil RA, Osman S, Pan J, Liu X, Wu Y. Recent progress on porous carbon derived from Zn and Al based metal-organic frameworks as advanced materials for supercapacitor applications. *J Energy Storage* **2021**;*44*:103263.

38. Hao L, Xia Q, Zhang Q, Masa J, Sun Z. Improving the performance of metal-organic frameworks for thermo-catalytic CO_2 conversion: strategies and perspectives. *Chinese J Catal* **2021**;*42*:1903–20.

39. El Hankari S, Bousmina M, El Kadib A. Biopolymer@Metal-Organic framework hybrid materials: a critical survey. *Prog Mater Sci* **2019**;*106*:100579.

40. Wu XP, Choudhuri I, Truhlar DG. Computational studies of photocatalysis with metal-organic frameworks. *Energy Environ Mater* **2019**;*2*:251–63.

41. Wei X, Song Y, Song L, Liu XD, Li Y, Yao S, et al. Phosphorization engineering on metal-organic frameworks for quasi-solid-state asymmetry supercapacitors. *Small* **2021**;*17*:2007062.

42. Yang XY, Li WJ, Tan ZL, Sha JQ, Tong ZB, Zhang Y, et al. Polyoxometalate-pillared metal-organic frameworks synthesized by surfactant-assisted strategy and incorporated with carbon nanotubes for energy storage. *J Mater Chem A* **2020**;*8*:25316–22.

43. Li C, Zhao DH, Long HL, Li M. Recent advances in carbonized non-noble metal–organic frameworks for electrochemical catalyst of oxygen reduction reaction. *Rare Met* **2021**;*40*:2657–89.

44. Geng P, Wang L, Du M, Bai Y, Li W, Liu Y, et al. MIL-96-Al for Li–S batteries: shape or size? *Adv Mater* **2022**;*34*:2107836.

45. Li W, Guo X, Geng P, Du M, Jing Q, Chen X, et al. Rational design and general synthesis of multimetallic metal-organic framework nano-octahedra for enhanced Li–S battery. *Adv Mater* **2021**;*33*:2105163.

46. Liu C, Bai Y, Li W, Yang F, Zhang G, Pang H. In Situ growth of three-dimensional MXene/metal–organic framework composites for high-performance supercapacitors. *Angew Chem Int Ed* **2022**;*61*:e202116282.

47. Bai Y, Liu C, Chen T, Li W, Zheng S, Pi Y, et al. MXene-copper/cobalt hybrids via Lewis acidic molten salts etching for high performance symmetric supercapacitors. *Angew Chem Int Ed* **2021**;*60*:25318–22.

48. Li X, Wei J, Li Q, Zheng S, Xu Y, Du P, et al. Nitrogen-doped cobalt oxide nanostructures derived from cobalt-alanine complexes for high-performance oxygen evolution reactions. *Adv Funct Mater* **2018**;*28*:1800886.

49. Li B, Gu P, Feng Y, Zhang G, Huang K, Xue H, et al. Ultrathin nickel-cobalt phosphate 2D nanosheets for electrochemical energy storage under aqueous/solid-state electrolyte. *Adv Funct Mater* **2017**;*27*:1605784.

50. Zheng S, Li Q, Xue H, Pang H, Xu Q. A highly alkaline-stable metal oxide@metal-organic framework composite for high-performance electrochemical energy storage. *Natl Sci Rev* **2020**;*7*:305–14.

51. Makhanya N, Oboirien B, Ren J, Musyoka N, Sciacovelli A. Recent advances on thermal energy storage using metal-organic frameworks (MOFs). *J Energy Storage* **2021**;*34*:102179.

52. Mohamed AM, Ramadan M, Allam NK. Recent advances on zeolitic imidazolate -67 metal-organic framework-derived electrode materials for electrochemical supercapacitors. *J Energy Storage* **2021**;*34*:102195.

53. Ubaidullah M, Al-Enizi AM, Ahamad T, Shaikh SF, Al-Abdrabalnabi MA, Samdani MS, et al. Fabrication of highly porous N-doped mesoporous carbon using waste polyethylene terephthalate bottle-based MOF-5 for high performance supercapacitor. *J Energy Storage* **2021**;*33*:102125.

54. Chen D, Wei L, Li J, Wu Q. Nanoporous materials derived from metal-organic framework for supercapacitor application. *J Energy Storage* **2020**;*30*:101525.

55. Mehtab T, Yasin G, Arif M, Shakeel M, Korai RM, Nadeem M, et al. Metal-organic frameworks for energy storage devices: batteries and supercapacitors. *J Energy Storage* **2019**;*21*:632–46.

56. Sankar SS, Karthick K, Sangeetha K, Karmakar A, Madhu R, Kundu S. Current perspectives on 3D ZIFs incorporated with 1D carbon matrices as fibers via electrospinning processes towards electrocatalytic water splitting: a review. *J Mater Chem A* **2021**;*9*:11961–2002.

57. Wang L, Li J, Cheng L, Song Y, Zeng P, Wen X. Application of hard and soft acid base theory to uncover the destructiveness of Lewis bases to UiO-66 type metal organic frameworks in aqueous solutions. *J Mater Chem A* **2021**;*9*:14868–76.

58. Xu LH, Li SH, Mao H, Zhang AS, Cai WW, Wang T, et al. An advanced necklace-like metal organic framework with an ultrahighly continuous structure in the membrane for superior butanol/water separation. *J Mater Chem A* **2021**;*9*:11853–62.

59. Moghadam PZ, Fairen-Jimenez D, Snurr RQ. Efficient identification of hydrophobic MOFs: application in the capture of toxic industrial chemicals. *J Mater Chem A* **2015**;*4*:529–36.

60. Tian HR, Zhang Z, Liu SM, Dang TY, Li XH, Lu Y, et al. A novel polyoxovanadate-based Co-MOF: highly efficient and selective oxidation of a mustard gas simulant by two-site synergetic catalysis. *J Mater Chem A* **2020**;*8*:12398–405.

61. Sánchez-González E, Mileo PGM, Sagastuy-Breña M, Álvarez JR, Reynolds JE, Villarreal A, et al. Highly reversible sorption of H_2S and CO_2 by an environmentally friendly Mg-based MOF. *J Mater Chem A* **2018**;*6*:16900–9.

62. Li J, Jiao C, Zhu J, Zhong L, Kang T, Aslam S, et al. Hybrid co-based MOF nanoboxes/CNFs interlayer as microreactors for polysulfides-trapping in lithium-sulfur batteries. *J Energy Chem* **2021**;*57*:469–76.

63. Khodayari P, Jalilian N, Ebrahimzadeh H, Amini S. Trace-level monitoring of anti-cancer drug residues in wastewater and biological samples by thin-film solid-phase micro-extraction using electrospun polyfam/Co-MOF-74 composite nanofibers prior to liquid chromatography analysis. *J Chromatogr A* **2021**;*1655*:462484.

64. Peng J, Tao J, Liu Z, Yang Y, Yu L, Zhang M, et al. Ultra-stable and high capacity flexible lithium-ion batteries based on bimetallic MOFs derivatives aiming for wearable electronic devices. *Chem Eng J* **2021**;*417*:129200.

65. Niu Q, Guo J, Chen B, Nie J, Guo X, Ma G. Bimetal-organic frameworks/polymer core-shell nanofibers derived heteroatom-doped carbon materials as electrocatalysts for oxygen reduction reaction. *Carbon* **2017**;*114*:250–60.

66. Piri-Moghadam H, Alam MN, Pawliszyn J. Review of geometries and coating materials in solid phase microextraction: opportunities, limitations, and future perspectives. *Anal Chim Acta* **2017**;*984*:42–65.

67. Efome JE, Rana D, Matsuura T, Lan CQ. Insight studies on metal-organic framework nanofibrous membrane adsorption and activation for heavy metal ions removal from aqueous Solution. *ACS Appl Mater Interfaces* **2018**;*10*:18619–29.

68. Topuz F, Abdulhamid MA, Hardian R, Holtzl T, Szekely G. Nanofibrous membranes comprising intrinsically microporous polyimides with embedded metal–organic frameworks for capturing volatile organic compounds. *J Hazard Mater* **2022**;*424*:127347.

69. Li XY, Yan Y, Zhang B, Bai TJ, Wang ZZ, He TS. PAN-derived electrospun nanofibers for supercapacitor applications: ongoing approaches and challenges. *J Mater Sci* **2021**;*56*:10745–81.

70. Acatay K, Simsek E, Ow-Yang C, Menceloglu YZ. Tunable, superhydrophobically stable polymeric surfaces by electrospinning. *Angew Chem Int Ed* **2004**;*43*:5210–3.

71. Giebel E, Mattheis C, Agarwal S, Greiner A. Chameleon nonwovens by green electrospinning. *Adv Funct Mater* **2013**;*23*:3156–63.

72. Greiner A, Wendorff JH. Electrospinning: a fascinating method for the preparation of ultrathin fibers. *Angew Chem Int Ed* **2007**;*46*:5670–703.

73. Li J, Song X, Zhang W, Xu H, Guo T, Zhang X, et al. Microporous carbon nanofibers derived from poly(acrylonitrile-co-acrylic acid) for high-performance supercapacitors. *Chem Eur J* **2020**;*26*:3326–34.

74. Liu Z, Fan X, Cheng L, Zhang J, Tang L, Tang Y, et al. Hybrid polymer membrane functionalized PBO fibers/cyanate esters wave-transparent laminated composites. *Adv Fiber Mater* **2022**;*4*:520–31.

75. Subjalearndee N, He N, Cheng H, Tesatchabut P, Eiamlamai P, Limthongkul P, et al. Gamma(γ)-MnO₂/rGO fibered cathode fabrication from wet spinning and dip coating techniques for cable-shaped Zn-ion batteries. *Adv Fiber Mater* **2022**;*4*:457–74.

76. Han J, Li L, Fang P, Guo R. Ultrathin MnO₂ nanorods on conducting polymer nanofibers as a new class of hierarchical nanostructures for high-performance supercapacitors. *J Phys Chem C* **2012**;*116*:15900–7.

77. Fan L, Yang L, Ni X, Han J, Guo R, Zhang C. Nitrogen-enriched meso-macroporous carbon fiber network as a binder-free flexible electrode for supercapacitors. *Carbon* **2016**;*107*:629–37.

78. Chen M, Wang C, Fang W, Wang J, Zhang W, Jin G, et al. Electrospinning of calixarene-functionalized polyacrylonitrile nanofiber membranes and application as an adsorbent and catalyst support. *Langmuir* **2013**;*29*:11858–67.

79. Lu L, Wu D, Zhang M, Zhou W. Fabrication of polylactide/poly(ε-caprolactone) blend fibers by electrospinning: Morphology and orientation. *Ind Eng Chem Res* **2012**;*51*:3682–91.

80. Zheng N, Huang Y, Sun W, Du X, Liu HY, Moody S, et al. In-situ pull-off of ZnO nanowire from carbon fiber and improvement of interlaminar toughness of hierarchical ZnO nanowire/carbon fiber hybrid composite laminates. *Carbon* **2016**;*110*:69–78.

81. González-Vila Á, Debliquy M, Lahem D, Zhang C, Mégret P, Caucheteur C. Molecularly imprinted electropolymerization on a metal-coated optical fiber for gas sensing applications. *Sens Actuators B Chem* **2017**;*244*:1145–51.

82. Chen J, Lu L, Wu D, Yuan L, Zhang M, Hua J, et al. Green poly(ε-caprolactone) composites reinforced with electrospun polylactide/poly(ε-caprolactone) blend fiber mats. *ACS Sustain Chem Eng* **2014**;*2*:2102–10.

83. Yu X, Pei C, Chen W, Feng L. 2 dimensional WS₂ tailored nitrogen-doped carbon nanofiber as a highly pseudocapacitive anode material for lithium-ion battery. *Electrochim Acta* **2018**;*272*:119–26.

84. Liu W, Wang S, Wu Q, Huan L, Zhang X, Yao C, et al. Fabrication of ternary hierarchical nanofibers MnO₂/PANI/CNT and theirs application in electrochemical supercapacitors. *Chem Eng Sci* **2016**;*156*:178–85.

85. Zhang Y, Wen F, Jiang Y, Wang L, Zhou C, Wang H. Layer-by-layer construction of caterpillar-like reduced graphene oxide-poly(aniline-co-o-aminophenol)-Pd nanofiber on glassy carbon electrode and its application as a bromate sensor. *Electrochim Acta* **2014**;*115*:504–10.

86. Ni Y, Liao Y, Zheng M, Shao S. In-situ growth of Co₃O₄ nanoparticles on mesoporous carbon nanofibers: a new nanocomposite for nonenzymatic amperometric sensing of H₂O₂. *Microchim Acta* **2017**;*184*:3689–95.

87. Yu L, Zhang Q, Xu Q, Jin D, Jin G, Li K, et al. Electrochemical detection of nitrate in PM2.5 with a copper-modified carbon fiber micro-disk electrode. *Talanta* **2015**;*143*:245–53.

88. Wang Q, Fang Z, Zhang W, Zhang D. High-efficiency g-C₃N₄ based photocatalysts for CO₂ reduction: modification methods. *Adv Fiber Mater* **2022**;*4*:342–60.

89. Song Q, Wu W, Wang Y, Yu J, Hu Z, Wang Y. The structure and properties of polyethylene oxide reinforced poly(Metaphenylene Isophthalamide) fibers. *Adv Fiber Mater* **2021**;*4*:436–47.

90. Qiu W, Liu XY. Recent progress of applying mesoscopic functionalization engineering principles to spin advanced regenerated silk fibroin fibers. *Adv Fiber Mater* **2022**;*4*:390–403.

91. Zhang M, Sun Q, Wang Y, Shan W, Lou Z, Xiong Y. Synthesis of porous UiO-66-NH₂-based mixed matrix membranes with high stability, flux and separation selectivity for Ga(III). *Chem Eng J* **2021**;*421*:129748.

92. Dai Z, Long Z, Li R, Shi C, Qiao H, Wang K, et al. Metal-organic framework-structured porous ZnCo₂O₄/C composite nanofibers for high-rate lithium-ion batteries. *ACS Appl Energy Mater* **2020**;*3*:12378–84.

93. Liu W, Zhang H, Zhang W, Wang M, Li J, Zhang Y, et al. Surface modification of a polylactic acid nanofiber membrane by zeolitic imidazolate framework-8 from secondary growth for drug delivery. *J Mater Sci* **2020**;*55*:15275–87.

94. Peng L, Zhang X, Sun Y, Xing Y, Li C. Heavy metal elimination based on metal organic framework highly loaded on flexible nanofibers. *Environ Res* **2020**;*188*:109742.

95. Yang X, Wu X, Chen Z, Li W, Sun QJ, Guo Z, et al. Hierarchically porous N-doped carbon nanofibers derived from ZIF-8/PAN composites for benzene adsorption. *J Appl Polym Sci* **2021**;*138*:50431.

96. Yang S, Cheng Y, Xiao X, Pang H. Development and application of carbon fiber in batteries. *Chem Eng J* **2020**;*384*:123294.

97. Li J, Zhang W, Zhang X, Huo L, Liang J, Wu L, et al. Copolymer derived micro/meso-porous carbon nanofibers with vacancy-type defects for high-performance supercapacitors. *J Mater Chem A* **2020**;*8*:2463–71.

98. Zhao J, He J, Sun M, Qu M, Pang H. Nickel hydroxide-nickel nanohybrids indirectly from coordination microfibers for high performance supercapacitor electrodes. *Inorg Chem Front* **2015**;*2*:129–35.

99. Liu X, Miao J, Fan Q, Zhang W, Zuo X, Tian M, et al. Recent progress on smart fiber and textile based wearable strain sensors: materials, fabrications and applications. *Adv Fiber Mater* **2022**;*4*:361–89.

100. Li L, Liu Y, Song C, Sheng S, Yang L, Yan Z, et al. Wearable alignment-free microfiber-based sensor chip for precise vital signs monitoring and cardiovascular assessment. *Adv Fiber Mater* **2022**;*4*:475–86.

101. Kang S, Zhao K, Guang D, Zheng X, Huang C. Advances in biosensing and environmental monitoring based on electrospun nanofibers. *Adv Fiber Mater* **2022**;*4*:404–35.

102. Armstrong MR, Arredondo KYY, Liu CY, Stevens JE, Mayhob A, Shan B, et al. UiO-66 MOF and poly(vinyl cinnamate) nanofiber composite membranes synthesized by a facile three-stage process. *Ind Eng Chem Res* **2015**;*54*:12386–92.

103. Dai X, Cao Y, Shi X, Wang X. The PLA/ZIF-8 nanocomposite membranes: the diameter and surface roughness adjustment by ZIF-8 nanoparticles, high wettability, improved mechanical property, and efficient oil/water separation. *Adv Mater Interfaces* **2016**;*3*:1600725.

104. Wu YN, Li F, Liu H, Zhu W, Teng M, Jiang Y, et al. Electrospun fibrous mats as skeletons to produce free-standing MOF membranes. *J Mater Chem* **2012**;*22*:16971–8.

105. Gao M, Zeng L, Nie J, Ma G. Polymer-metal-organic framework core-shell framework nanofibers: Via electrospinning and their gas adsorption activities. *RSC Adv* **2016**;*6*:7078–85.

106. He XX, Zheng J, Yu GF, You MH, Yu M, Ning X, et al. Near-field electrospinning: progress and applications. *J Phys Chem C* **2017**;*121*:8663–78.

107. Ji D, Peng S, Fan L, Li L, Qin X, Ramakrishna S. Thin MoS₂ nanosheets grafted MOFs-derived porous Co-N-C flakes grown on electrospun carbon nanofibers as self-supported bifunctional catalysts for overall water splitting. *J Mater Chem A* **2017**;*5*:23898–908.

108. Li T, Zhang Z, Han Z. Research progress in polymer-based metal-organic framework nanofibrous membranes based on electrospinning. *J Inorg Mater* **2021**;*36*:592–600.

109. Liu C, Wang J, Li J, Liu J, Wang C, Sun X, et al. Electrospun ZIF-based hierarchical carbon fiber as an efficient electrocatalyst for the oxygen reduction reaction. *J Mater Chem A* **2017**;*5*:1211–20.

110. Jiang S, Hou H, Agarwal S, Greiner A. Polyimide nanofibers by "green" electrospinning via aqueous solution for filtration applications. *ACS Sustain Chem Eng* **2016**;*4*:4797–804.

111. Jung JW, Lee CL, Yu S, Kim ID. Electrospun nanofibers as a platform for advanced secondary batteries: a comprehensive review. *J Mater Chem A* **2016**;*4*:703–50.

112. Luo CJ, Stoyanov SD, Stride E, Pelan E, Edirisinghe M. Electrospinning versus fibre production methods: from specifics to technological convergence. *Chem Soc Rev* **2012**;*41*:4708–35.

113. Deng N, Wang L, Feng Y, Liu M, Li Q, Wang G, et al. Co-based and Cu-based MOFs modified separators to strengthen the kinetics of redox reaction and inhibit lithium-dendrite for long-life lithium-sulfur batteries. *Chem Eng J* **2020**;*388*:124241.

114. Jiang S, Chen Y, Duan G, Mei C, Greiner A, Agarwal S. Electrospun nanofiber reinforced composites: a review. *Polym Chem* **2018**;*9*:2685–720.

115. Zhang CL, Jiang ZH, Lu BR, Liu JT, Cao FH, Li H, et al. MoS$_2$ nanoplates assembled on electrospun polyacrylonitrile-metal organic framework-derived carbon fibers for lithium storage. *Nano Energy* **2019**;*61*:104–10.

116. Song J, Huang M, Lin X, Li SFY, Jiang N, Liu Y, et al. Novel Fe-based metal–organic framework (MOF) modified carbon nanofiber as a highly selective and sensitive electrochemical sensor for tetracycline detection. *Chem Eng J* **2021**;*427*:130913.

117. Bhardwaj N, Kundu SC. Electrospinning: a fascinating fiber fabrication technique. *Biotechnol Adv* **2010**;*28*:325–47.

118. Liu M, Cai N, Chan V, Yu F. Development and applications of MOFs derivative one-dimensional nanofibers via electrospinning: a mini-review. *Nanomaterials* **2019**;*9*:1306.

119. Dou Y, Zhang W, Kaiser A. Electrospinning of metal-organic frameworks for energy and environmental applications. *Adv Sci* **2020**;*7*:1902590.

120. Wang C, Kaneti YV, Bando Y, Lin J, Liu C, Li J, et al. Metal-organic framework-derived one-dimensional porous or hollow carbon-based nanofibers for energy storage and conversion. *Mater Horizons* **2018**;*5*:394–407.

121. Lu AX, McEntee M, Browe MA, Hall MG, Decoste JB, Peterson GW. MOFabric: electrospun nanofiber mats from PVDF/UiO-66-NH$_2$ for chemical protection and decontamination. *ACS Appl Mater Interfaces* **2017**;*9*:13632–6.

122. Liang H, Yao A, Jiao X, Li C, Chen D. Fast and sustained degradation of chemical warfare agent simulants using flexible self-supported metal-organic framework filters. *ACS Appl Mater Interfaces* **2018**;*10*:20396–403.

123. Fan L, Xue M, Kang Z, Li H, Qiu S. Electrospinning technology applied in zeolitic imidazolate framework membrane synthesis. *J Mater Chem* **2012**;*22*:25272–6.

124. Guo J, Gao M, Nie J, Yin F, Ma G. ZIF-67/PAN-800 bifunctional electrocatalyst derived from electrospun fibers for efficient oxygen reduction and oxygen evolution reaction. *J Colloid Interface Sci* **2019**;*544*:112–20.

125. Li Z, Chen B, Wang X, Nie J, Ma G. Electrospun bamboo-like Fe$_3$C encapsulated Fe-Si-N co-doped nanofibers for efficient oxygen reduction. *J Colloid Interfac Sci* **2019**;*546*:231–9.

126. Hao Z, Wu J, Wang C, Liu J. Electrospun polyimide/metal-organic framework nanofibrous membrane with superior thermal stability for efficient PM2.5 capture. *ACS Appl Mater Interfaces* **2019**;*11*:11904–9.

127. El-Aswar EI, Ramadan H, Elkik H, Taha AG. A comprehensive review on preparation, functionalization and recent applications of nanofiber membranes in wastewater treatment. *J Environ Manage* **2022**;*301*:113908.

128. Li X, Zhou R, Wang Z, Zhang M, He T. Electrospun metal-organic framework based nanofibers for energy storage and environmental applications: current approaches and challenges. *J Mater Chem A* **2022**;*10*:1642–81.

129. Zhao J, Gong B, Nunn WT, Lemaire PC, Stevens EC, Sidi FI, et al. Conformal and highly adsorptive metal-organic framework thin films via layer-by-layer growth on ALD-coated fiber mats. *J Mater Chem A* **2015**;*3*:1458–64.

130. Di J, Guo J, Wang N, Ma G. Multicomponent doped sugar-coated haws stick-like nanofibers as efficient oxygen reduction reaction catalysts for the Zn-Air battery. *ACS Sustain Chem Eng* **2019**;*7*:7716–27.

131. Mallakpour S, Sirous F, Hussain CM. Metal-organic frameworks/biopolymer nanocomposites: from fundamentals toward recent applications in modern technology. *New J Chem* **2021**;*45*:8409–26.

132. Zhao G, Zhao H, Zhuang X, Shi L, Cheng B, Xu X, et al. Nanofiber hybrid membranes: progress and application in proton exchange membranes. *J Mater Chem A* **2021**;*9*:3729–66.

133. Wang C, Zheng T, Luo R, Liu C, Zhang M, Li J, et al. In situ growth of ZIF-8 on PAN fibrous filters for highly efficient U(VI) removal. *ACS Appl Mater Interfaces* **2018**;*10*:24164–71.

134. Bian Y, Wang R, Wang S, Yao C, Ren W, Chen C, et al. Metal-organic framework-based nanofiber filters for effective indoor air quality control. *J Mater Chem A* **2018**;*6*:15807–14.

135. Zhao R, Tian Y, Li S, Ma T, Lei H, Zhu G. An electrospun fiber based metal-organic framework composite membrane for fast, continuous, and simultaneous removal of insoluble and soluble contaminants from water. *J Mater Chem A* **2019**;*7*:22559–70.

136. Lu AX, Ploskonka AM, Tovar TM, Peterson GW, Decoste JB. Direct surface growth of UIO-66-NH$_2$ on polyacrylonitrile nanofibers for efficient toxic chemical removal. *Ind Eng Chem Res* **2017**;*56*:14502–6.

137. Jin R, Bian Z, Li J, Ding M, Gao L. ZIF-8 crystal coatings on a polyimide substrate and their catalytic behaviours for the Knoevenagel reaction. *Dalt Trans* **2013**;*42*:3936–40.

138. Lian Z, Huimin L, Zhaofei O. In situ crystal growth of zeolitic imidazolate frameworks(ZIF)on electrospun polyurethane nanofibers. *Dalt Trans* **2014**;*43*:6684–8.

139. Li Z, Zhou G, Dai H, Yang M, Fu Y, Ying Y, et al. Biomineralization-mimetic preparation of hybrid membranes with ultra-high loading of pristine metal-organic frameworks grown on silk nanofibers for hazard collection in water. *J Mater Chem A* **2018**;*6*:3402–13.

140. Li H, Zhu L, Zhang J, Guo T, Li X, Xing W, et al. High-efficiency separation performance of oil-water emulsions of polyacrylonitrile nanofibrous membrane decorated with metal-organic frameworks. *Appl Surf Sci* **2019**;*476*:61–9.

141. Azadmanjiri J, Srivastava VK, Kumar P, Nikzad M, Wang J, Yu A. Two- and three-dimensional graphene-based hybrid composites for advanced energy storage and conversion devices. *J Mater Chem A* **2018**;*6*:702–34.

142. Fang Y, Ma Y, Zheng M, Yang P, Asiri AM, Wang X. Metal–organic frameworks for solar energy conversion by photoredox catalysis. *Coord Chem Rev* **2018**;*373*:83–115.

143. Gür TM. Review of electrical energy storage technologies, materials and systems: Challenges and prospects for large-scale grid storage. *Energy Environ Sci* **2018**;*11*:2696–767.

144. Guo Q, Li Y, Wei XY, Zheng LW, Li ZQ, Zhang KG, et al. Electrospun metal-organic frameworks hybrid nanofiber membrane for efficient removal of As(III) and As(V) from water. *Ecotoxicol Environ Saf* **2021**;*228*:112990.

145. Kang Z, Fan L, Sun D. Recent advances and challenges of metal-organic framework membranes for gas separation. *J Mater Chem A* **2017**;*5*:10073–91.

146. Qian Q, Asinger PA, Lee MJ, Han G, Mizrahi Rodriguez K, Lin S, et al. MOF-based membranes for gas separations. *Chem Rev* **2020**;*120*:8161–266.

147. Tee JK, Yip LX, Tan ES, Santitewagun S, Prasath A, Ke PC, et al. Nanoparticles' interactions with vasculature in diseases. *Chem Soc Rev* **2019**;*48*:5381–407.

148. Zheng Q, Shen H, Shuai D. Emerging investigators series: advances and challenges of graphitic carbon nitride as a visible-light-responsive photocatalyst for sustainable water purification. *Environ Sci Water Res Technol* **2017**;*3*:982–1001.

149. Huang A, Ma Y, Peng J, Li L, Chou S, Ramakrishna S, et al. Tailoring the structure of silicon-based materials for lithium-ion batteries via electrospinning technology. *eScience* **2021**;*1*:141–62.

150. Deng L, Hu F, Ma M, Huang SC, Xiong Y, Chen HY, et al. Electronic modulation caused by interfacial Ni-O-M (M=Ru, Ir, Pd) bonding for accelerating hydrogen evolution kinetics. *Angew Chem Int Ed* **2021**;*60*:22276–82.

151. Hao Y, Hu F, Chen Y, Wang Y, Xue J, Yang S, et al. Recent progress of electrospun nanofibers for zinc-air batteries. *Adv Fiber Mater* **2022**;*4*:185–202.

152. Huang H, Yu D, Hu F, Huang SC, Song J, Chen HY, et al. Clusters induced electron redistribution to tune oxygen reduction activity of transition metal single-atom for metal-air batteries. *Angew Chem Int Ed* **2022**;*61*:e202116068.

153. Li L, Yu D, Li P, Huang H, Xie D, Lin CC, et al. Interfacial electronic coupling of ultrathin transition-metal hydroxide nanosheets with layered MXenes as a new prototype for platinum-like hydrogen evolution. *Energy Environ Sci* **2021**;*14*:6419–27.

154. Song J, Qiu S, Hu F, Ding Y, Han S, Li L, et al. Sub-2 nm thiophosphate nanosheets with heteroatom doping for enhanced oxygen electrocatalysis. *Adv Funct Mater* **2021**;*31*:2100618.

155. Liang C, Chen J, Yu K, Jin W. $ZnMn_2O_4$ spheres anchored on jute porous carbon for use as a high-performance anode material in lithium-ion batteries. *J Alloys Compd* **2021**;*878*:160445.

156. Wang X, Fang Y, Yan X, Liu S, Zhao X, Zhang L. Highly conductive polymer electrolytes based on PAN-PEI nanofiber membranes with in situ gelated liquid electrolytes for lithium-ion batteries. *Polymer* **2021**;*230*:124038.

157. Zhu S, Sun J, Wu T, Su X, Su H, Qu S, et al. Graphitized porous carbon nanofibers prepared by electrospinning as anode materials for lithium ion batteries. *RSC Adv* **2016**;*6*:83185–95.

158. Zhu S, Chen M, Sun J, Liu J, Wu T, Su H, et al. Novel highly conductive ferroferric oxide/porous carbon nanofiber composites prepared by electrospinning as anode materials for high performance Li-ion batteries. *RSC Adv* **2016**;*6*:58529–40.

159. Xu Z, Fan L, Ni X, Han J, Guo R. Sn-encapsulated N-doped porous carbon fibers for enhancing lithium-ion battery performance. *RSC Adv* **2019**;*9*:8753–8.

160. Ge P, Zhang L, Yang Y, Sun W, Hu Y, Ji X. Advanced $MoSe_2$/carbon electrodes in Li/Na-ions batteries. *Adv Mater Interfaces* **2020**;*7*:1901651.

161. Huang TT, Wu W. Scalable nanomanufacturing of inkjet-printed wearable energy storage devices. *J Mater Chem A* **2019**;*7*:23280–300.

162. Li Y, Li Q, Tan Z. A review of electrospun nanofiber-based separators for rechargeable lithium-ion batteries. *J Power Sources* **2019**;*443*:227262.

163. Chen YM, Yu L, Lou XW. Hierarchical tubular structures composed of Co_3O_4 hollow nanoparticles and carbon nanotubes for lithium storage. *Angew Chem Int Ed* **2016**;*55*:5990–3.

164. Wu N, Wang J, Liao C, Han L, Song L, Hu Y, et al. A flame retardant separator modified by MOFs-derived hybrid for safe and efficient Li-S batteries. *J Energy Chem* **2022**;*64*:372–84.

165. Choi S, Song J, Wang C, Park S, Wang G. Multifunctional free-standing gel polymer electrolyte with carbon nanofiber interlayers for high-performance lithium-sulfur batteries. *Chem-Asian J* **2017**;*12*:1470–4.

166. Ni L, Zhao G, Wang Y, Wu Z, Wang W, Liao Y, et al. Coaxial carbon/MnO_2 hollow nanofibers as sulfur hosts for high-performance lithium-sulfur batteries. *Chem-Asian J* **2017**;*12*:3128–34.

167. Xiao P, Xu Y. Recent progress in two-dimensional polymers for energy storage and conversion: design, synthesis, and applications. *J Mater Chem A* **2018**;*6*:21676–95.

168. An Y, Tan S, Liu Y, Zhu K, Hu L, Rong Y, et al. Designs and applications of multi-functional covalent organic frameworks in rechargeable batteries. *Energy Storage Mater* **2021**;*41*:354–79.

169. Zhou Z, Li G, Zhang J, Zhao Y. Wide working temperature range rechargeable lithium-sulfur batteries: a critical review. *Adv Funct Mater* **2021**;*31*:2107136.

170. Lee J, Lee T, Char K, Kim KJ, Choi JW. Issues and advances in scaling up sulfide-based all-solid-state batteries. *Acc Chem Res* **2021**;*54*:3390–402.

171. Ren YX, Zhao TS, Liu M, Tan P, Zeng YK. Modeling of lithium-sulfur batteries incorporating the effect of Li_2S precipitation. *J Power Sources* **2016**;*336*:115–25.

172. Kosasang S, Ma N, Duangdangchote S, Chiochan P, Chanlek N, Sawangphruk M. Strong cooperative interaction of lithium and hydrogen bonds between 4-aminobenzoic acid modified interlayer and polysulfides for lithium-sulfur batteries. *Carbon* **2019**;*155*:553–61.

173. Niu H, Wang L, Guan P, Zhang N, Yan C, Ding M, et al. Recent advances in application of ionic liquids in electrolyte of lithium ion batteries. *J Energy Storage* **2021**;*40*:102659.

174. Zhao Y, Zhang ZL, Ling XY, Xu XJ, Ma LF, Pang H. Intercalation pseudocapacitance in ZnS@C sheets composites for enhanced electrochemical energy storage. *J Energy Storage* **2021**;*39*:102611.

175. Abdul Razzaq A, Yuan X, Chen Y, Hu J, Mu Q, Ma Y, et al. Anchoring MOF-derived CoS_2 on sulfurized polyacrylonitrile nanofibers for high areal capacity lithium-sulfur batteries. *J Mater Chem A* **2020**;*8*:1298–306.

176. Wei J, Jiang C, Chen B, Li X, Zhang H. Hollow C/Co_9S_8 hybrid polyhedra-modified carbon nanofibers as sulfur hosts for promising Li–S batteries. *Ceram Int* **2021**;*47*:25387–97.

177. Liu Y, Zhong W, Yang C, Pan Q, Li Y, Wang G, et al. Direct synthesis of FeS/N-doped carbon composite for high-performance sodium-ion batteries. *J Mater Chem A* **2018**;*6*:24702–8.

178. Wu Y, Fan X, Gaddam RR, Zhao Q, Yang D, Sun X, et al. Mesoporous niobium pentoxide/carbon composite electrodes for sodium-ion capacitors. *J Power Sources* **2018**;*408*:82–90.

179. Zhou G, Miao YE, Wei Z, Mo LL, Lai F, Wu Y, et al. Bioinspired micro/nanofluidic ion transport channels for organic cathodes in high-rate and ultrastable lithium/sodium-ion batteries. *Adv Funct Mater* **2018**;*28*:1804629.

180. Hao Z, Dimov N, Chang JK, Okada S. Tin phosphide-carbon composite as a high-performance anode active material for sodium-ion batteries with high energy density. *J Energy Chem* **2022**;*64*:463–74.

181. Senthil C, Park JW, Shaji N, Sim GS, Lee CW. Biomass seaweed-derived nitrogen self-doped porous carbon anodes for sodium-ion batteries: Insights into the structure and electrochemical activity. *J Energy Chem* **2021**;*64*:286–95.

182. Sun C, Zhang X, Li C, Wang K, Sun X, Liu F, et al. A safe, low-cost and high-efficiency presodiation strategy for pouch-type sodium-ion capacitors with high energy density. *J Energy Chem* **2022**;*64*:442–50.

183. Wu H, Zhang X, Wu Q, Han Y, Wu X, Ji P, et al. Confined growth of 2D MoS_2 nanosheets in N-doped pearl necklace-like structured carbon nanofibers with boosted lithium and sodium storage performance. *Chem Commun* **2020**;*56*:141–4.

184. Aguesse F, Lopez del Amo JM, Otaegui L, Goikolea E, Rojo T, Singh G. Structural and electrochemical analysis of Zn doped $Na_3Ni_2SbO_6$ cathode for Na-ion battery. *J Power Sources* **2016**;*336*:186–95.

185. Wu X, Li Y, Xiang Y, Liu Z, He Z, Wu X, et al. The electrochemical performance of aqueous rechargeable battery of Zn/Na0.44MnO2 based on hybrid electrolyte. *J Power Sources* **2016**;*336*:35–9.

186. Fu L, Xiong W, Liu Q, Wan S, Kang C, Li G, et al. Metalorganic framework derived FeS/MoS_2 composite as a high performance anode for sodium-ion batteries. *J Alloys Compd* **2021**;*869*:159348.

187. Jiang Y, Xie M, Wu F, Ye Z, Zhang Y, Wang Z, et al. Cobalt selenide hollow polyhedron encapsulated in graphene for high-performance lithium/sodium storage. *Small* **2021**;*17*:2102893.

188. Peng J, Ou M, Yi H, Sun X, Zhang Y, Zhang B, et al. Defect-free-induced Na^+ disordering in electrode materials. *Energy Environ Sci* **2021**;*14*:3130–40.

189. Guo Y, Zhu Y, Yuan C, Wang C. $MgFe_2O_4$ hollow microboxes derived from metal-organic-frameworks as anode material for sodium-ion batteries. *Mater Lett* **2017**;*199*:101–4.

190. Shao M, Cheng Y, Zhang T, Li S, Zhang W, Zheng B, et al. Designing MOFs-derived FeS_2@carbon composites for high-rate sodium ion storage with capacitive contributions. *ACS Appl Mater Interfaces* **2018**;*10*:33097–104.

191. Sridhar V, Park H. Microwave induced transformation of metal organic frameworks into defect rich carbon nanofibers. *New J Chem* **2020**;*44*:5666–72.

192. Yang X, Wang S, Yu DYW, Rogach AL. Direct conversion of metal-organic frameworks into selenium/selenide/carbon composites with high sodium storage capacity. *Nano Energy* **2019**;*58*:392–8.

193. Zhang W, Yue Z, Wang Q, Zeng X, Fu C, Li Q, et al. Carbon-encapsulated CoS_2 nanoparticles anchored on N-doped carbon nanofibers derived from ZIF-8/ZIF-67 as anode for sodium-ion batteries. *Chem Eng J* **2020**;*380*:122548.

194. Wang Y, Wen Z, Wang CC, Yang CC, Jiang Q. MOF-derived Fe_7S_8 nanoparticles/N-doped carbon nanofibers as an ultra-stable anode for sodium-ion batteries. *Small* **2021**;*17*:2102349.

195. Das R, Vecitis CD, Schulze A, Cao B, Ismail AF, Lu X, et al. Recent advances in nanomaterials for water protection and monitoring. *Chem Soc Rev* **2017**;*46*:6946–7020.

196. Li X, Gao X, Ai L, Jiang J. Mechanistic insight into the interaction and adsorption of Cr(VI) with zeolitic imidazolate framework-67 microcrystals from aqueous solution. *Chem Eng J* **2015**;*274*:238–46.

197. Ding M, Bannuru KKR, Wang Y, Guo L, Baji A, Yang HY. Free-standing electrodes derived from metal-organic frameworks/ nanofibers hybrids for membrane capacitive deionization. *Adv Mater Technol* **2018**;*3*:1800135.

198. Xu S, Ren LF, Zhou Q, Bai H, Li J, Shao J. Facile ZIF-8 functionalized hierarchical micronanofiber membrane for high-efficiency separation of water-in-oil emulsions. *J Appl Polym Sci* **2018**;*135*:46462.

199. Huang X, Zhang S, Xiao W, Luo J, Li B, Wang L, et al. Flexible PDA@ACNTs decorated polymer nanofiber composite with superhydrophilicity and underwater superoleophobicity for efficient separation of oil-in-water emulsion. *J Memb Sci* **2020**;*614*:118500.

200. Wu W, Shi N, Zhang J, Wu X, Wang T, Yang L, et al. Electrospun fluorescent sensors for the selective detection of nitro explosive vapors and trace water. *J Mater Chem A* **2018**;*6*:18543–50.

201. Gao J, Li B, Wang L, Huang X, Xue H. Flexible membranes with a hierarchical nanofiber/microsphere structure for oil adsorption and oil/water separation. *J Ind Eng Chem* **2018**;*68*:416–24.

202. Gupta RK, Dunderdale GJ, England MW, Hozumi A. Oil/water separation techniques: A review of recent progresses and future directions. *J Mater Chem A* **2017**;*5*:16025–58.

203. Ma Q, Yu Y, Sindoro M, Fane AG, Wang R, Zhang H. Carbon-based functional materials derived from waste for water remediation and energy storage. *Adv Mater* **2017**;*29*:1605361.

204. Li K, Ju J, Xue Z, Ma J, Feng L, Gao S, et al. Structured cone arrays for continuous and effective collection of micron-sized oil droplets from water. *Nat Commun* **2013**;*4*:2276.

205. Chen X, Chen D, Li N, Xu Q, Li H, He J, et al. Modified-MOF-808-loaded polyacrylonitrile membrane for highly efficient, simultaneous emulsion separation and heavy metal ion removal. *ACS Appl Mater Interfaces* **2020**;*12*:39227–35.

206. Hou X, Zhou H, Zhang J, Cai Y, Huang F, Wei Q. High adsorption pearl-necklace-like composite membrane based on metal-organic framework for heavy metal ion removal. *Part Part Syst Charact* **2018**;*35*:1700438.

207. Lin S, Song Z, Che G, Ren A, Li P, Liu C, et al. Adsorption behavior of metal-organic frameworks for methylene blue from aqueous solution. *Microporous Mesoporous Mater* **2014**;*193*:27–34.

208. Zhu Z, Bai YL, Zhang L, Sun D, Fang J, Zhu S. Two nanocage anionic metal–organic frameworks with rht topology and $([M(H_2O)_6]_6)^{12+}$ charge aggregation for rapid and selective adsorption of cationic dyes. *Chem Commun* **2014**;*50*:14674–7.

209. Wang XS, Liang J, Li L, Lin ZJ, Bag PP, Gao SY, et al. An anion metal-organic framework with Lewis basic sites-rich toward charge-exclusive cationic dyes separation and size-selective catalytic reaction. *Inorg Chem* **2016**;*55*:2641–9.

210. Hasan Z, Jhung SH. Removal of hazardous organics from water using metal-organic frameworks (MOFs): plausible mechanisms for selective adsorptions. *J Hazard Mater* **2015**;*283*:329–39.

211. Yao S, Xu T, Zhao N, Zhang L, Huo Q, Liu Y. An anionic metal-organic framework with ternary building units for rapid and selective adsorption of dyes. *Dalt Trans* **2017**;*46*:3332–7.

212. Li T, Liu L, Zhang Z, Han Z. Preparation of nanofibrous metal-organic framework filter for rapid adsorption and selective separation of cationic dye from aqueous solution. *Sep Purif Technol* **2020**;*237*:116360.

213. Dai X, Li X, Zhang M, Xie J, Wang X. Zeolitic imidazole framework/graphene oxide hybrid functionalized poly(lactic acid) electrospun membranes: a promising environmentally friendly water treatment material. *ACS Omega* **2018**;*3*:6860–6.

214. Chen L, Wang X, Rao Z, Tang Z, Wang Y, Shi G, et al. In-situ synthesis of Z-Scheme MIL-100(Fe)/α-Fe_2O_3 heterojunction for enhanced adsorption and visible-light photocatalytic oxidation of O-xylene. *Chem Eng J* **2021**;*416*:129112.

215. Liu B, Younis SA, Kim KH. The dynamic competition in adsorption between gaseous benzene and moisture on metal-organic frameworks across their varying concentration levels. *Chem Eng J* **2021**;*421*:127813.

216. Ibrahim AO, Adegoke KA, Adegoke RO, AbdulWahab YA, Oyelami VB, Adesina MO. Adsorptive removal of different pollutants using metal-organic framework adsorbents. *J Mol Liq* **2021**;*333*:115593.

217. Wen J, Fang Y, Zeng G. Progress and prospect of adsorptive removal of heavy metal ions from aqueous solution using metal–organic frameworks: a review of studies from the last decade. *Chemosphere* **2018**;*201*:627–43.

218. Wang B, Xie LH, Wang X, Liu XM, Li J, Li JR. Applications of metal–organic frameworks for green energy and environment: new advances in adsorptive gas separation, storage and removal. *Green Energy Environ* **2018**;*3*:191–228.

219. Lee M, Ojha GP, Oh HJ, Kim T, Kim HY. Copper//terbium dual metal organic frameworks incorporated side-by-side electrospun nanofibrous membrane: a novel tactics for an efficient adsorption

of particulate matter and luminescence property. *J Colloid Interface Sci* **2020**;*578*:155–63.

220. Wang X, Xu W, Gu J, Yan X, Chen Y, Guo M, et al. MOF-based fibrous membranes adsorb PM efficiently and capture toxic gases selectively. *Nanoscale* **2019**;*11*:17782–90.

221. Zhang Y, Yuan S, Feng X, Li H, Zhou J, Wang B. Preparation of nanofibrous metal−organic framework filters for. *J Am Chem Soc* **2016**;*138*:5785–8.

222. Liu C, Jiang Y, Zhou C. Photo-switchable smart metal–organic framework membranes with tunable and enhanced molecular sieving performance. *J Mater Chem A* **2018**;*6*:24949–55.

223. Zhang Y, Yang L, Wang L, Cui X, Xing H. Pillar iodination in functional boron cage hybrid supramolecular frameworks for high performance separation of light hydrocarbons. *J Mater Chem A* **2019**;*7*:27560–6.

224. Jiamjirangkul P, Inprasit T, Intasanta V, Pangon A. Metal organic framework-integrated chitosan/poly (vinyl alcohol) (PVA) nanofibrous membrane hybrids from green process for selective CO_2 capture and filtration. *Chem Eng Sci* **2020**;*221*:115650.

225. Zhang Y, Zhang Y, Wang X, Yu J, Ding B. Ultrahigh metal−organic framework loading and flexible nanofibrous membranes for efficient CO_2 capture with long-term, ultrastable recyclability. *ACS Appl Mater Interfaces* **2018**;*10*:34802–10.

Publisher's Note Springer Nature remains neutral with regard to jurisdictional claims in published maps and institutional affiliations.

Huan Pang received his Ph. D. degree from Nanjing University in 2011. He is now a distinguished professor at Yangzhou University and a Young Changjiang Scholar of the Ministry of Education in China. He is a senior member of the Chinese Chemical Society. He is the managing editor of Energy-Chem, the editorial board member of FlatChem and Rare Metals, and the youth editorial board member of Nano Research, Nano Research Energy, eScience, Advanced Fiber Materials among other distinguished academic journals. He was recognized as a highly cited researcher in Cross-Field by Clarivate Analytics in 2020 and 2021. He has won "Best Editor Award 2021" for his professional excellence and outstanding contribution to Nano Research. His research area mainly focuses on metal–organic frameworks (MOFs) related materials.